Characterizing the Size and Composition of Saposin A Lipoprotein Picodiscs

Jun Li,[1] Michele R. Richards,[1] Dhanashri Bagal,[2] Iain D. G. Campuzano,[2] Elena N. Kitova,[1] Zi Jian Xiong,[3] Gilbert G. Privé,[3,4] and John S. Klassen[1*]

[1]*Alberta Glycomics Centre and Department of Chemistry, University of Alberta, Edmonton, Alberta, Canada T6G 2G2*

[2]*Amgen, Discovery Analytical Sciences, Thousand Oaks, California, United States 91320*

[3]*Department of Biochemistry, University of Toronto, Toronto, Ontario, Canada M5S 1A8*

[4] *Princess Margaret Cancer Centre, University Health Network, Toronto, Ontario, Canada M5G 1L7*

*Email: john.klassen@ualberta.ca

Abstract

Saposin A (SapA) lipoprotein discs, also known as picodiscs (PDs), represent an attractive method to solubilize glycolipids for protein interaction studies in aqueous solution. Recent electrospray ionization mass spectrometry (ESI-MS) data suggest that the size and composition of 1-palmitoyl-2-oleoyl-*sn*-glycero-3-phosphocholine (POPC)-containing PDs at neutral pH differs from those of *N*,*N*-dimethyldodecylamine *N*-oxide determined by X-ray crystallography. Using high resolution ESI-MS, multi-angle laser light scattering (MALLS) and molecular dynamics (MD) simulations, the composition, heterogeneity and structure of POPC-PDs in aqueous ammonium acetate solutions at pH 4.8 and 6.8 were investigated. The ESI-MS and MALLS data revealed that POPC-PDs consist predominantly of (SapA dimer + *i*POPC) complexes, with i = 23 to 29, and have an average molecular weight (MW) of 38.2 ± 3.3 kDa at pH 4.8. In contrast, in freshly prepared solutions at pH 6.8, POPC-PDs are composed predominantly of (SapA tetramer + *i*POPC) complexes, with i = 37 to 60, with an average MW of 68.0 ± 2.7 kDa. However, the (SapA tetramer + *i*POPC) complexes are unstable at neutral pH and convert, over a period of hours, to (SapA trimer + *i*POPC) complexes, with i = 29 to 36, with an average MW of 51.1 ± 2.9 kDa. The results of molecular modelling suggest spheroidal structures for the (SapA dimer + *i*POPC), (SapA trimer + *i*POPC) and (SapA tetramer + *i*POPC) complexes in solution. Comparison of measured collision cross sections (Ω) with values calculated for gaseous (SapA dimer + 26POPC)$^{8+}$, (SapA trimer + 33POPC)$^{12+}$ and (SapA tetramer + 42POPC)$^{16+}$ ions produced from modelling suggests that the solution structures are largely preserved in the gas phase, although the lipids do not maintain regular bilayer orientations.

Introduction

Protein interactions with glycolipids (GLs) present in the plasma membrane represent an important class of recognition events that are implicated in a wide variety of cellular processes, including cell-cell adhesion, signalling, immune response and pathogen infection.[1–4] Although the biological importance of protein−GL binding is well established, the identification of the functional GL receptors for many proteins, including bacterial and viral lectins, and the characterization of these interactions is challenging. The detection of protein−GL interactions is commonly performed using techniques such as enzyme-linked immunosorbent assay (ELISA), surface plasmon resonance (SPR) spectroscopy, thin-layer chromatography (TLC) with immuno-overlay or microarrays of naturally-occurring or synthetic GLs.[5,6] A potential limitation of these surface-based approaches is that protein−GL binding may be affected by the nature of the surface coupling (immobilization), GL density, the loss of mobility and the orientation of the carbohydrate moiety in the immobilized GLs.[7]

An alternative strategy to probe protein−GL interactions is to present the GLs in a lipid environment. A number of different model membranes have been used for such purposes, including supported lipid bilayers, liposomes, micelles and nanodiscs (NDs).[8–11] Recently, the use of saposin A (SapA)-containing discs to solubilize GLs and present them for protein binding studies was reported.[12,13] These binding studies were carried out using the catch-and-release electrospray ionization-mass spectrometry (Car-ESI-MS) assay.[12,13] Saposin A, a sphingolipid activator protein involved in the transport and degradation of galactosylceramide by lysosomal hydrolases,[14–15] is a small (molecular weight (MW) ~9 kDa) alpha helical protein that, upon incubation with detergent or lipid, self-assembles into disc-like structures.[15] These SapA discs, which are also referred to as picodiscs (PDs), share some structural similarities with NDs (which

are ~150 kDa water-soluble discoidal (diameter ~10 nm) phospholipid bilayers surrounded by two copies of an amphipathic membrane scaffold protein (MSP)),[10] but are reported to be smaller in physical size and MW.[15] According to a reported crystal structure (PDB ID: 4ddj), SapA discs of *N*,*N*-dimethyldodecylamine *N*-oxide (LDAO) are composed of two SapA and forty detergent molecules (twenty-four and sixteen LDAO per leaflet), with a MW ~27 kDa.[15] In the presence of liposomes of the phospholipid 1-palmitoyl-2-oleoyl-*sn*-glycero-3-phosphocholine (POPC, Figure S1, Supporting Information) at pH 4.8, which is the expected pH within lysosomes, discs with hydrodynamic radii of ~3.2 nm, MWs of 35-45 kDa (determined by size exclusion chromatography (SEC)) and a 5:1 ratio of lipid/SapA have been detected.[15]

Picodiscs have been shown to be attractive alternatives to NDs for the presentation of GLs for protein binding studies *in vitro*, particularly for low affinity interactions.[12,13] For example, the weak interaction ($(0.27 \pm 0.08) \times 10^3$ M^{-1})[16] between the B subunit homopentamer of shiga toxin type 1 and a known cellular receptor, the globotriaosylceramide Gb3, was successfully detected using ESI-MS and Gb3-containing PDs, but not with NDs.[12] Given the significant role that PDs are likely to play in the discovery and characterization of protein−GL interactions, there is a clear need to accurately establish the size and composition of lipid-PDs in aqueous solutions.[12,13] Here, we describe the results of a detailed investigation into the composition, heterogeneity and structure of POPC-containing PDs in aqueous ammonium acetate solutions at pH 4.8 and 6.8 using high resolution ESI-MS, multi-angle laser light scattering (MALLS) and molecular dynamics (MD) simulations. Collision cross sections (Ω) were also determined from ion mobility separation (IMS) measurements to assess the structures of PD ions in the gas phase.

Experimental Section

Proteins, Lipids and Detergent

Saposin A (SapA, which was produced as two major isoforms with MWs 8 918 Da and MW 9 049 Da), was expressed and purified as previously described.[15] Cytochrome c from equine heart (Cyt, MW 12 384 Da), transthyretin from human plasma (TTR, MW 56 kDa), and avidin from chicken egg white (Avidin, MW 64 kDa), which were used to construct the Ω calibration curve for IMS measurements, were purchased from Sigma-Aldrich Canada (Oakville, Canada). Stock solutions of Cyt, TTR and Avidin in 200 mM aqueous ammonium acetate were prepared by dissolving a known mass of protein. All stock solutions were stored at –20 °C until needed. The phospholipid POPC (MW 760.08 Da) was purchased from Avanti Polar Lipids Inc. (Alabaster, AL).

Picodisc Preparation

Picodiscs were prepared as previously described.[15] Briefly, POPC (dissolved in chloroform) alone was dried under nitrogen, and placed in a vacuum desiccator overnight to form a lipid film. The lipid film was then diluted in 50 mM sodium acetate and 150 mM sodium chloride (pH 4.8) to form liposomes by sonication and ~10 freeze/thaw cycles. Picodisc formation was initiated by the addition of SapA protein, at a 1:10 molar ratio of SapA to total lipid, followed by incubation at 37 °C for 45 min. Finally, PDs were purified using a Superdex 75 10/300 size exclusion column (GE Healthcare Bio-Sciences, Uppsala, Sweden) equilibrated in 50 mM sodium acetate and 150 mM sodium chloride (pH 4.8). The PD fractions were pooled, concentrated and buffer exchanged into 200 mM aqueous ammonium acetate (pH 6.8). PDs were concentrated to approximately 150 μM and stored at room temperature until used.

Mass Spectrometry

Mass spectrometry measurements were performed on an Exactive Plus (with extended mass range) Orbitrap Fourier-transform (FT) mass spectrometer (Thermo Fisher Scientific, Bremen, Germany)[17,18] and a Synapt G2S quadrupole-ion mobility separation-time-of-flight (Q-IMS-TOF) mass spectrometer (Waters, Manchester, UK). Both instruments were equipped with nanoflow ESI (nanoESI) sources. A brief overview of the instrumental conditions used is given below.

Exactive Plus Orbitrap. NanoESI, at a flow rate of about 1-2 μL h^{-1} using 4 μm id GlassTip Emitters (New Objective, Woburn, MA), was used to spray aqueous ammonium acetate (200 mM) solutions of PDs (5 μM). The capillary voltage was set to 1.8 kV; ions formed by nanoESI were sampled through a stainless steel capillary (ion transfer tube) maintained at 250 ^{o}C into an S-Lens stacked ring ion guide with an applied RF-amplitude (peak-to-peak) of 200 V. Ions then travel through a transport multipole and enter the HCD cell where they were stored at a high pressure before they were returned to the C-trap. This feature allows efficient trapping and desolvation of large protein ions and dramatically improves sensitivity. Transients detected were processed using enhanced Fourier transformation (eFT^{TM}) for converting the time domain into frequency domain and then into *m/z* values.[19] Data was analyzed using xcaliber^{TM}2.2. No additional data processing (smoothing) was performed. Spectral deconvolution was performed with the UniDec[20] deconvolution algorithm and a detailed description is given as Supporting Information.

Synapt G2S. Borosilicate capillaries (1.0 mm o.d., 0.68 mm i.d.) were pulled in-house using a P-1000 micropipette puller (Sutter Instruments, Novato, CA). A voltage of ~1.0 kV was applied to a platinum wire was inserted into the nanoESI tip. A source temperature of 60 °C and a cone

voltage 30 V were used. Argon was used in the Trap and Transfer ion guides at pressures of 2.77 x 10^{-2} mbar and 2.84 x 10^{-2} mbar, respectively, and the Trap and Transfer voltages were 5 V and 2 V, respectively. To dissociate PDs, the *m/z* region corresponding to PD ions were selected by quadrupole mass filter and subjected to collision-induced dissociation (CID) in the Trap region using a series of collision energies from 5 V to 100 V. For IMS, a wave height of 40 V and a wave velocity of 1000 m s^{-1} were applied along with a helium and nitrogen (IMS gas) gas flow of 50 and 60 mL min^{-1}, respectively. All data was processed using MassLynx software (*v*4.1) in combination with Driftscope *v*2.5.

Collision Cross Section Analysis

The Ω of the gaseous PD ions were determined from the IMS measurements using a protocol described elsewhere.[21,22] Briefly, the relationship between drift times (t_D) and Ω was established by analyzing calibrant proteins (Cyt, TTR and Avidin) with known Ω (in N_2) under the same experimental conditions. A detailed description of the procedure is given as Supporting Information.

Size-Exclusion Chromatography/Multi-Angle Laser Light Scattering (SEC-MALLS)

Picodiscs in 200 mM aqueous ammonium acetate (pH 4.8 or pH 6.8) were injected into a Superose^{TM} 12 HR 10/30 column, which was equilibrated using the same aqueous ammonium acetate solution. Picodisc elution was detected via refractive index using an in-line Optilab rEX^{TM} differential refractive index detector and DAWN EOS^{TM} MALLS, which includes both MALLS and Quasi-Elastic Light Scattering (QELS) detectors (Wyatt Technologies, Santa Barbara, CA). The combined MALLS-QELS can measure simultaneously radius of gyration (R_g, from 10-500 nm), hydrodynamic radius (R_h, from 1-500 nm) and MW. However, for PDs, the R_g was below the angular variation detection limit of 10 nm, so only R_h and MW were obtained.

Data were processed using ASTRA version 5.3.4.14 software. Average values of the MW and R_h for PDs were calculated form data collected over the elution peak and MW predictions were normalized to a BSA standard.

Molecular Dynamic (MD) Simulations

MD simulations were performed on four different POPC-containing PDs – (SapA dimer + 10POPC), (SapA dimer + 26POPC), (SapA trimer + 33POPC) and (SapA tetramer + 42POPC). Initial conformations for MD (Figure S4) were generated in Chimera[23] using SapA coordinates from Popovic *et al*. (PDB ID: 4ddj),[15] and various POPC bilayers generated using the membrane plugin for VMD.[24,25] The SapA proteins were manually placed around each bilayer to allow for minimal close contacts and minimal extra vacuum space (initial coordinates are included as Supporting Information). The MD simulations were performed in aqueous solution and the gas phase for all four systems using the AMBER12[26] software package. Simulations in aqueous solution were run in boxes of TIP3P[27] water using the PMEMD module in AMBER12 for 50 ns under NPT conditions at 1 atm and 300 K. The solution cut-off for nonbonding interactions was 8 Å. The gas-phase MD simulations were run using the SANDER module in AMBER12 for 20 ns at 300 K, with cut-off for nonbonding interactions set to 999 Å. For the gas-phase complexes, each SapA protein was at a +4 charge state. The positive charges were placed evenly over the surface of the protein with R68, K19, K33, and K40 protonated. The remaining lysine residues (K8, K48, and K63) were neutral, as were all aspartic acid and glutamic acid residues. The equilibrated structures from solution simulations were used as the initial structures for the gas-phase simulations. A detailed description of the parameters used for the simulations is given as Supporting Information.

Results and Discussion

a. Composition and size of POPC-PDs

To probe the composition and polydispersity of POPC-PDs in acidic and neutral solutions, ESI-MS measurements were carried out using both ToF-MS (Synapt G2S) and FT-MS (Exactive Plus Orbitrap). Shown in Figure 1 are representative ESI mass spectra acquired in positive mode for aqueous solutions of POPC-PD in 200 mM aqueous ammonium acetate, at pH 4.8 or pH 6.8, measured using the Synapt mass spectrometer. The mass spectrum shown in Figure 1a was acquired for a freshly prepared acidic (pH 4.8) solution containing 10 μM PD (the PD stock solution was diluted from 150 μM to a final concentration of 10 μM in the 200 mM aqueous ammonium acetate). Signal corresponding to protonated POPC and SapA monomer ions was detected, as well as a broad feature centred at *m/z* ~3500, which could not be fully resolved. All ions with *m/z* >2500 were selected using the quadrupole mass filter and simultaneously subjected to CID in the Trap region using a moderate (50 V) collision energy. Collisional activation, which caused the POPC-PDs signal to be distributed over a broader range of *m/z* values (with a shift towards higher *m/z*), resulted in peaks that were partially resolved. The peak identities were made based on the theoretical and measured *m/z* values (Table S1, Supporting Information). It should be noted that the SapA used to produce the PDs consists of two major isoforms (Figure S2). Consequently, the SapA dimer exists at three distinct MWs, corresponding to two homodimers and one heterodimer, while the SapA trimer exists at four MWs, corresponding to two homotrimers and two heterotrimers. Analysis of the mass spectrum revealed the presence of protonated ions of POPC, SapA monomer and the (SapA monomer + *i*POPC) complexes, where i = 1 to 3, at charge states +3 to +6, SapA dimer and the (SapA dimer + *i*POPC) complexes, where i = 1 to 4, at charge state +4 to +5, and the (SapA dimer + *i*POPC) complexes, where i = 23 to 28, at charge state +6 to +7, and the SapA trimer and (SapA trimer + *i*POPC) complexes,

where *i* = 1 to 2, at charge states +6 (Figure 1b). The presence of POPC-bound SapA dimer is consistent with the crystal structure reported for LDAO-PDs prepared at acidic pH.[15] However, the presence of free and POPC-bound SpaA trimer ions suggests that, at least, some fraction of the POPC-PDs at pH 4.8 exist as SapA trimers or larger multimers. Measurements carried out on the same solution as described above, but following incubation for 3 h at room temperature, revealed no significant differences (Figures 1c and 1d, Table S2, Supporting Information). This finding suggests that the POPC-PDs species are kinetically stable (over the timescale of the measurements) at acidic pH.

Measurements analogous to those described above were carried out on a freshly prepared neutral (pH 6.8) aqueous ammonium acetate solution containing 10 μM PD (Figure 1e). In addition to signal corresponding to protonated ions of POPC and SapA monomer, two broad features centred at *m/z* ~4000 and ~4300 were observed. CID (collision energy of 50 V in the Trap) performed on ions with *m/z* >3500 resulted in the appearance of POPC, SapA monomer and the (SapA monomer + *i*POPC) complex, where *i* = 1 to 4, at charge states +3 to +6, the (SapA trimer + *i*POPC) ions, where *i* = 19 to 29, at charge states +7 to +8 and/or the (SapA tetramer + *i*POPC) ions, where *i* = 37 to 45, at charge states +10 (Figure 1f, Table S3, Supporting Information). Notably, there was no evidence of ions corresponding to SapA dimer, either on its own or bound to POPC. These results suggest that the POPC-PDs do not exist as SapA dimer at neutral pH and, instead, contain ≥3 copies of SapA. Measurements performed on this same solution, but following incubation for 3 h, at room temperature revealed subtle changes in the relative abundance of the two broad features noted above (Figure 1g). Moreover, CID produced POPC, SapA monomer and the (SapA monomer + *i*POPC) complex, where *i* = 1 to 3, at charge states +3 to +6, and SapA trimer ions bound to a number of POPC, i.e., (SapA trimer + *i*POPC)

ions, where *i* = 20 to 28, at charge states +7 to +8 and/or (SapA trimer + *i*POPC) ions, where *i* = 27 to 35, at charge states +9 (Figure 1h, Table S4, Supporting Information). These results suggest that, upon dilution, the composition of the POPC-PDs in neutral solution changes with time, whereby tetrameric POPC-PDs convert to trimer.

In order to more precisely establish the composition and degree of heterogeneity of the POPC-PDs under acidic and neutral conditions, high resolution ESI-MS analysis was performed using FT-MS. Shown in Figure 2a is a representative ESI mass spectrum acquired for a freshly prepared 200 mM aqueous ammonium acetate solution, at pH 4.8, containing 5 µM PD; the mass spectrum shown in Figure 2d was acquired after 3 h at room temperature. An expanded view of the *m/z* 4400 – 5800 portions of the two mass spectra is given in Figure 2b and Figure 2e, respectively. In both Figure 2a and Figure 2d, the POPC dimer ion was detected, along with two distributions of ions corresponding to (SapA dimer + *i*POPC) complexes, where *i* = 23 to 29, at charge states +7 to +8. Shown in Figure 2c and Figure 2f are the zero-charge mass spectra corresponding to the mass spectral data shown in Figure 2a and Figure 2d, respectively. In addition to the dominant (SapA dimer + *i*POPC) species, with *i* = 23 to 29 and a weighted average MW of 38.2 ± 3.3 kDa, there is evidence of smaller (SapA dimer + *i*POPC) complexes, with *i* = 12 to 20, (SapA trimer + *i*POPC) complexes with *i* = 32 to 37, and (SapA tetramer + *i*POPC) complexes with *i* = 48 to 60. The zero-charge mass spectrum shown in Figure 2f, acquired after 3 h of incubation, revealed a similar distribution of species. This observation, which is consistent with results obtained by ToF-MS, suggests that the distribution of POPC-PD species remains relatively constant over time at acidic pH.

High resolution ESI mass spectra acquired for a 200 mM aqueous ammonium acetate solution (pH 6.8) of 5 µM PD POPC-PDs, acquired immediately after preparation and after 3 h

incubation, are shown in Figures 3a and 3d, respectively; expanded views of the region of the mass spectra containing signal for the POPC-PDs are given in Figure 3b (*m/z* 6200 – 7800) and Figure 3e (*m/z* 4200 – 6000), respectively. The corresponding zero-charge mass spectra are shown in Figure 3c and Figure 3f, respectively. Analysis of the mass spectral data suggests that, for the freshly prepared neutral solution, POPC-PDs exist predominantly as (SapA tetramer + *i*POPC) complexes with i = 37 to 47 and an average MW of 68.0 ± 2.7 kDa; (SapA tetramer + *i*POPC) complexes with i = 55 to 60 were also detected but at low abundance. After incubation for 3 h, there is an obvious change in the distribution of POPC-PD species – a significant fraction of the (SapA tetramer + *i*POPC) complexes appears to have transformed to (SapA trimer + *i*POPC) complexes, with i = 29 to 36 and an average MW of 51.1 ± 2.9 kDa (Figure 3f).

The size and MWs of the POPC-PDs in neutral and acidic solutions were also investigated using MALLS coupled with SEC. Shown in Figure S3 are the chromatograms and corresponding MW distributions acquired for 200 mM aqueous ammonium acetate solutions, at pH 4.8 (Figure S3a) or 6.8 (Figure S3b), containing 225 μM POPC-PDs. It can be seen that, at acidic pH, the POPC-PDs have MWs ranging from approximately 35 kDa to 50 kDa, with an average MW of 40.9 ± 1.6 kDa. These results are consistent with the values (35-45 kDa) estimated for POPC-PDs based on SEC measurements.[15] Of more significance, the average MW determined by MALLS is in good agreement with the value determined by ESI-MS (38.2 ± 3.3 kDa). It can also be seen from the MALLS data that POPC-PDs are more heterogeneous and span a much wider range of MWs (approximately 50 kDa to 90 kDa) at neutral pH, and have an average MW of 73.7 ± 0.4 kDa. This average MW is in good agreement with the value of 68.0 ± 2.7 kDa determined by ESI-MS performed on the freshly prepared POPC-PD solution. It can be concluded, therefore, that, at neutral pH, POPC-PDs exist predominantly as (SapA tetramer +

*i*POPC) complexes. As described above, the ESI-MS data suggest that the (SapA tetramer + *i*POPC) complexes are unstable at neutral pH and, over a period of hours, convert to (SapA trimer + *i*POPC) complexes. In addition to providing insight into the MWs of the POPC-PDs, the MALLS data also provide an estimate of R_h. According to the measured data, the POPC-PDs have an R_h of 31.0 ± 1.5 Å at acidic pH and an R_h of 39.0 ± 0.2 Å at neutral pH. The value measured at pH 4.8 agrees with the R_h value (32.5 Å) reported previously.[15]

b. Structures of POPC-PDs in solution

A series of MD simulations were performed with the goal of estimating the solution structures of the different POPC-PD species identified by ESI-MS and MALLS. The simulations were carried out with four different species – (SapA dimer + 10POPC), (SapA dimer + 26POPC), (SapA trimer + 33POPC) and (SapA tetramer + 42POPC). The initial structure of the (SapA dimer + 10POPC) complex was based on the reported model for POPC-PDs (Figure S4).[15] Initial structures for the other three complexes, which are among the most abundant species detected by ESI-MS, were built by manually arranging SapA proteins around a bilayer of POPC (Figure S4). Analysis of the 50-ns simulations performed on the hydrated POPC-PDs shows that, while the complexes undergo a slight compaction, the POPCs remain in a bilayer-like arrangement throughout the simulation (Figure 4). The R_g values of the four POPC-PD complexes were monitored over the course of the simulation and found to remain relatively constant; with average values of 17.6 ± 0.2 Å (SapA dimer + 10POPC), 20.6 ± 0.2 Å (SapA dimer + 26POPC), 23.3 ± 0.3 Å (SapA trimer + 33POPC), and 26.0 ± 0.2 Å (SapA tetramer + 42POPC) (Table 1 and Figure S5, Supporting Information).

As described above, R_g values for the POPC-PDs could not be measured using MALLS. Consequently, a direct comparison of the R_g values determined from the structures generated

from modelling with experimental values was not possible. The R_g/R_h ratios, based on the R_g values calculated for the (SapA dimer + 26POPC) and (SapA tetramer + 42POPC) complexes and the experimental R_h values determined at pH 4.8 and 6.8 are 0.66–0.67 (Table 1). These values are somewhat smaller than the theoretical value of 0.775 expected for hard spheres.[33] However, it is known that core weighting of the density distributions of spheres, as might be expected in the case of the PDs, leads to R_g/R_h ratios <0.775.[28] Moreover, the ratios calculated for the POPC-PDs are similar to values (0.68–0.69) reported for poly(amidoamine) (PAMAM) dendrimers of comparable size (e.g. R_g = 17.1 Å and 26.3 Å for generation 4 and 6).[29] While the aforementioned analysis does not enable any conclusions to be drawn regarding the shapes (structures) of the solvated POPC-PDs, it does raise the possibility that the (SapA dimer + *i*POPC), (SapA tetramer + *i*POPC) and, presumably, (SapA trimer + *i*POPC) complexes adopt spheroidal structures, of the type shown in Figure 4, in solution.

c. Structures of POPC-PDs in the gas phase

It is also relevant, in the context of the CaR-ESI-MS assay, to ask what happens to the structures of the POPC-PD complexes once they are transferred to the gas phase. As a step towards answering this question, Ω values of the gaseous POPC-PD ions produced by ESI were determined by measuring the IMS drift times and comparing those values with drift times measured for calibrant protein ions (with known Ω values). The corresponding calibration plot, produced using Cyt, TTR and Avidin, is shown in Figure S6 (Supporting Information). It can be seen that there is a linear correlation (correlation coefficient (R^2) of 0.996) between the drift times (corrected drift times, t_D'') and known Ω values. Shown in Figure S7 are the ESI mass spectra and the corresponding 3D IMS heat maps (*m/z* versus IMS drift times) measured for POPC-PD ions produced from 200 mM ammonium acetate aqueous solutions at pH 4.8 (Figures

S7a and S7b) or 6.8 (Figures S7c and S7d). The results shown in Figure S7a and Figure S7c were acquired immediately after preparing the POPC-PD solutions; those shown in Figure S7b and Figure S7d were acquired following 3 h incubation. Listed in Tables S5, S6, S7 (Supporting Information) are the Ω values for the POPC-PD ions determined from their corrected drift times (t_D'') and the calibration curve shown in Figure S6 (Supporting Information).

Summarized in Table 2 are the average Ω values of gaseous POPC-PD ions, taken over all compositions and all charge states. It can be seen that, as expected, Ω scales with the number of SapA proteins contained in the POPOC-PD ions. The (SapA dimer + *i*POPC) complexes with i = 23 to 29, the dominant species in acidic solution, have an average Ω of 29.5 ± 0.6 nm^2. The (SapA tetramer + *i*POPC) complexes with i = 37 to 47, which are dominant in freshly diluted solution at neutral pH, have an average Ω of 48.6 ± 1.1 nm^2, while the (SapA trimer + *i*POPC) complexes with i = 29 to 36, which dominate at longer times, have an average Ω of 37.1 ± 0.7 nm^2. Shown in Figure S8 (Supporting Information) are the measured Ω values plotted versus composition (number of POPC) at given charge states. It can also be seen that, for POPC-PDs with the same charge state, Ω increases, approximately linearly, with the number of POPCs. On average (considering all POPC-PD ions), Ω increases by 0.25 ± 0.12 nm^2 per POPC; for (SapA dimer + *i*POPC) ions (i = 24 to 29), Ω increases by 0.22 ± 0.10 nm^2 per POPC at charge states +10 and +11 (Table S5, Supporting Information); for (SapA trimer + *i*POPC) ions Ω increases by 0.25 ± 0.14 nm^2 per POPC at charge state +12 and +13 (Table S7, Supporting Information); for the (SapA tetramer + *i*POPC) ions Ω increases by 0.28 ± 0.11 nm^2 per POPC at charge states +14 to +17 (Table S6, Supporting Information).

In order to interpret the Ω data acquired for the gaseous POPC-PD ions, MD simulations were performed on the $(SapA\ dimer + 26POPC)^{8+}$, $(SapA\ trimer + 33POPC)^{12+}$, and (SapA

tetramer + 42POPC)$^{16+}$ ions. All of the POPC-PD ions maintain a spheroidal shape, similar to the solutions structures, throughout the simulation, although the lipids do not maintain regular bilayer orientations, especially on the edges of the lipid packet (Figures S9 and S10, Supporting Information). The gaseous ions also tend to be slightly more compact than their solution counterparts. For example, the average R_g for (SapA dimer + 26POPC)$^{8+}$ and (SapA tetramer + 42POPC)$^{16+}$ ions are 0.7 Å smaller than the solution complexes; the (SapA trimer + 33POPC)$^{12+}$ ion has the same average R_g, within error, as the hydrated complex (Figures S5 and S11, Supporting Information). Theoretical values of Ω were also calculated for averaged structures of gaseous POPC-PD complexes over the course of the simulations. The theoretical Ω for the gas-phase (SapA dimer + 26POPC)$^{8+}$, (SapA trimer + 33POPC)$^{12+}$, and (SapA tetramer + 42POPC)$^{16+}$ ions are 31.5 nm^2, 41.8 nm^2, and 49.3 nm^2, respectively (Table 2). Notably, these values are within 12% of the average experimental Ω values determined for POPC-PDs with the same composition (29.3 ± 0.9 nm^2, 37.4 ± 0.6 nm^2 and 49.4 ± 0.6 nm^2, respectively, Table 2) and within 15% of the average values at all measured compositions (29.5 ± 0.6 nm^2, 37.1 ± 0.7 nm^2 and 48.6 ± 1.1 nm^2, respectively). These results suggest that the calculated structures, in particular those of (SapA dimer + 26POPC)$^{8+}$ and (SapA tetramer + 42POPC)$^{16+}$, might provide a reasonable representation of the structures of the POPC-PD ions in the gas phase.

Conclusions

The results of the first detailed investigation into the size and composition of POPC-PDs in neutral and acidic solution are reported. The ESI-MS and MALLS data acquired at pH 4.8 revealed that POPC-PDs consist predominantly of (SapA dimer + *i*POPC) complexes, where *i* = 23 to 29, and have an average MW of 38.2 ± 3.3 kDa and an average R_h of 31.0 ± 1.5 Å. In contrast, data acquired at pH 6.8 revealed that, in freshly prepared solutions, POPC-PDs exist

predominantly as (SapA tetramer + *i*POPC) complexes, where i = 37 to 60, and have an average MW of 68.0 ± 2.7 kDa and an average R_h of 39.0 ± 0.2 Å. It was also found that the (SapA tetramer + *i*POPC) complexes convert, over a period of hours, to (SapA trimer + *i*POPC) complexes, with i = 29 to 36 and an average MW of 51.1 ± 2.9 kDa. At present, the mechanism underlying this conversion process is not understood and will be the focus of future study. The results of molecular modelling suggest spheroidal structures for the (SapA dimer + *i*POPC), (SapA trimer + *i*POPC) and (SapA tetramer + *i*POPC) complexes in solution. Comparison of experimentally determined Ω with values calculated for gaseous $(\text{SapA dimer + 26POPC})^{8+}$, $(\text{SapA trimer + 33POPC})^{12+}$ and $(\text{SapA tetramer + 42POPC})^{16+}$ ions produced from modelling suggests that the solution structures are largely preserved in the gas phase, although the lipids do not maintain regular bilayer orientations. Finally, it should be noted that the results of this study lay the foundation for future investigations into the structures of GL-loaded PDs and their use in protein−GL interaction studies.

ASSOCIATED CONTENT

Supporting Information

Mass spectra, IMS arrival times, structures, trajectories and experimental details. This information is available free of charge via the Internet at http://pubs.acs.org/.

Author Information

Corresponding Author

john.klassen@ualberta.ca

Notes

The authors declare no competing financial interests.

Acknowledgements

The authors are grateful for financial support provided by the National Sciences and Research Council of Canada and the Alberta Glycomics Centre (J.S.K.) and the Canadian Institutes of Health Research (G.G.P.).

References

1. Malhotra, R. *Biochem. Anal. Biochem.* **2012**, *1*, 108.
2. Hakomori, S. *Curr. Opin. Hematol.* **2003**, *10*, 16−24.
3. Sharon, N.; Lis, H. *Sci. Am*. **1993**, *268*, 82−89.
4. Varki, A.; Cummings, R. D.; Esko, J. D.; Freeze, H. H.; Stanley, P.; Bertozzi, C. R.; Hart, G. W.; Etzler, M. E. *Essentials of Glycobiology*, 2nd ed.; Cold Spring Harbor Laboratory Press: Cold Spring Harbor, NY, 2009.
5. Lopez, H. H. H.; Schnaar, R. L. *Methods Enzymol*. **2006**, *417*, 205–220.
6. Feizi, T. *Ann. N.Y. Acad. Sci*. **2013**, *1292*, 33−44.
7. Grant, O. C.; Smith, H. M.; Firsova, D.; Fadda, E.; Woods, R. J. *Glycobiology* **2014**, *24*, 17−25.
8. Shi, J.; Yang, T.; Kataoka, S.; Zhang, Y.; Diaz, A. J.; Cremer, P. S. *J. Am. Chem. Soc*. **2007**, *129*, 5954−5961.
9. Jayaraman, N.; Maiti, K.; Naresh, K. *Chem. Soc. Rev*. **2013**, *42*, 4640 −4656.
10. Bayburt, T. H.; Grinkova, Y. V.; Sligar, S. G. *Nano Lett*. **2002**, *2*, 853−856.
11. Zhang, Y.; Liu, L.; Daneshfar, R.; Kitova, E. N.; Li, C.; Jia, F.; Cairo, C.W.; Klassen, J. S. *Anal. Chem.* **2012**, *84*, 7618−7621.
12. Leney, A. C.; Darestani, R. R.; Li, J.; Nikjah, S.; Kitova, E. N.; Zou, C.; Cairo, C. W.; Xiong, Z. J.; Privé, G. G.; Klassen, J. S. *Anal. Chem.* **2015**, *87*, 4402−4408.
13. Li, J.; Fan, X.; Kitova, E. N.; Zou, C.; Cairo, C. W.; Eugenio, L.; Ng, K. K. S.; Xiong, Z. J.; Privé, G. G.; Klassen, J. S. *Anal. Chem.* **2016**, *88*, 4742-4750.
14. Locatelli-Hoops, S.; Remmel, N.; Klingenstein, R.; Breiden, B.; Rossocha, M. Schoeniger, M.; Koenigs, C.; Saenger, W.; Sandhoff, K. *J. Biol. Chem*. **2006**, *281*, 32451.

15. Popovic, K.; Holyoake, J.; Pomès, R.; Privé, G. G. *Prot. Natl. Acad. Sci.* **2012**, *109*, 2908−2912.

16. Sun, J.; Kitova, E.N.; Wang, W.; Klassen, J. S. *Anal. Chem.* **2006**, *78*, 3010−3018.

17. Rose, R. J.; Damoc, E,; Denisov, E.; Makarov, A.; Heck, A. J. R. *Nat. Methods* **2012**, *9*, 1084−1086.

18. Rosati, S.; Rose, R. J.; Thompson, N. J.; Van Duijn, E.; Damoc, E.; Denisov, E.; Makarov, A.; Heck, A. J. *Angew. Chem. Int. Ed*. **2012**, *51*, 12992−12996.

19. Michalski, A.; Damoc, E.; Hauschild, J. P.; Lange, O.; Wieghaus, A.; Makarov, A.; Nagaraj, N.; Cox, J.; Mann, M.; Horning, S. *Mol. Cell. Proteomics*. **2011**, *10*, M111.011015.

20. Marty, M. T.; Baldwin, A. J.; Marklund, E. G.; Hochberg, G. K.; Benesch, J. L.; Robinson, C. V. *Anal. Chem.* **2015**, *87*, 4370-4376.

21. Bush, M. F.; Hall, Z.; Giles, K.; Hoyes, J.; Robinson, C. V.; Ruotolo, B. T. *Anal. Chem*. **2010**, *82*, 9557−9565.

22. Ruotolo, B. T.; Benesch, J. L. P.; Sandercock, A. M.; Hyung, S. J.; Robinson, C. V. *Nat. Protoc*. **2008**, *3*, 1139−1152.

23. Pettersen, E. F.; Goddard, T. D.; Huang, C. C.; Couch, G. S.; Greenblatt, D. M.; Meng, E. C.; Ferrin, T. E. *J. Comput. Chem.* **2004**, *25*, 1605–1612.

24. Balabin, I. Membrane Plugin, Version 1.1. http://www.ks.uiuc.edu/Research/vmd/plugins/membrane/ (accessed 11/21/2014).

25. Humphrey, W.; Dalke, A.; Schulten, K. *J. Mol. Graphics* **1996**, *14*, 33–38.

26. Case, D. A.; Darden, T. A.; Cheatham III, T. E.; Simmerling, C. L.; Wang, J.; Duke, R. E.; Luo, R.; Walker, R. C.; Zhang, W.; Merz, K. M.; Roberts, B.; Hayik, S.; Roitberg, A.;

Seabra, G.; Swails, J.; Götz, A. W.; Kolossváry, I.; Wong, K. F.; Paesani, F.; Vanicek, J.; Wolf, R. M.; Liu, J.; Wu, X.; Brozell, S. R.; Steinbrecher, T.; Gohlke, H.; Cai, Q.; Ye, X.; Wang, J.; Hsieh, M.-J.; Cui, G.; Roe, D. R.; Mathews, D. H.; Seetin, M. G.; Salomon-Ferrer, R.; Sagui, C.; Babin, V.; Luchko, T.; Gusarov, S.; Kovalenko, A.; Kollman, P. A. AMBER 12, University of California: San Fancisco, CA, 2012.

27. Jorgensen, W. L.; Chandrasekhar, J.; Madura, J. D.; Impey, R. W.; Klein, M. L. *J. Chem. Phys.* **1983**, *79*, 926–935.

28. Antonietti, M.; Bremser, W.; Schmidt, M. *Macromolecules* **1990**, *23*, 3796−3805.

29. Tande, B. M.; Wagner, N. J.; Mackay, M. E.; Hawker, C. J.; Jeong, M. *Macromolecules* **2001**, *34*, 8580−8585.

Table 1. Solution properties of POPC-PD species evaluated by ESI-MS, SEC-MALLS, and MD simulations.[a]

POPC-PD	*i*	Average MW (kDa)	Measured R_h (Å)	Average R_g (Å)	R_g/R_h
(SapA dimer + *i*POPC)	10	ND	ND	17.6 ± 0.2 [d]	ND
(SapA dimer + *i*POPC)	23-29 [b]	38.2 ± 3.3 [b] 40.9 ± 1.6 [c]	31.0 ± 1.5 [c]	20.6 ± 0.2 [d] (*i* = 26)	0.66 [e]
(SapA trimer + *i*POPC)	29-36 [b]	51.1 ± 2.9 [b]	ND	23.3 ± 0.3 [d] (*i* = 33)	ND
(SapA tetramer + *i*POPC)	37-47 [b]	68.0 ± 2.7 [b] 73.7 ± 0.4 [c]	39.0 ± 0.2 [c]	26.0 ± 0.2 [d] (*i* = 42)	0.67 [e]

a. ND ≡ Not determined. b. Values measured by FT-MS. c. Values measured by SEC-MALLS. d. Values calculated by MD simulations in solution and averaged over 50 ns. e. Ratio of calculated R_g to measured R_h.

Table 2. Collision cross sections (Ω) of POPC-PD species from ESI-IMS-MS measurements and MD simulations.

POPC-PD	Measured Ω (nm^2) [a,b]	Measured Ω (nm^2) [a]	Calculated Ω (nm^2) [c]
(SapA dimer + *i*POPC)	29.5 ± 0.6 (*i* = 23-29)	29.3 ± 0.9 (*i* = 26)	31.5 (*i* = 26)
(SapA trimer + *i*POPC)	37.1 ± 0.7 (*i* = 29-36)	37.4 ± 0.6 (*i* = 33)	41.8 (*i* = 33)
(SapA tetramer + *i*POPC)	48.6 ± 1.1 (*i* = 37-47)	49.4 ± 0.6 (*i* = 42)	49.3 (*i* = 42)

a. Values measured by ESI-IMS-MS. b. Values averaged over all measured compositions. c. Value calculated for averaged structure from MD simulations.

Figure captions

Figure 1. ESI mass spectra acquired by ToF-MS in positive ion mode for freshly prepared 200 mM aqueous ammonium acetate solutions of POPC-PDs (10 μM) at (a) pH 4.8 or (e) pH 6.8. (b) and (f) CID mass spectra (50 V in Trap) for the POPC-PD ions produced from the solutions described in (a) and (e), respectively. (c) and (g) ESI mass spectra acquired for the solutions described in (a) and (e), respectively, after 3 h incubation. (d) and (h) CID mass spectra (50 V in Trap) for POPC-PD ions produced from the solutions described in (c) and (g), respectively.

Figure 2. ESI mass spectra acquired by FT-MS in positive ion mode for a 200 mM aqueous ammonium acetate solution of POPC-PDs (5 μM) at pH 4.8 (a) immediately after preparation of the solution and (d) after 3 h incubation. (b) and (e) Expanded view of the mass spectra shown in (a) and (d), respectively. (c) and (f) Zero-charge mass spectrum corresponding to (a) and (d), respectively.

Figure 3. ESI mass spectra acquired by FT-MS in positive ion mode for a 200 mM aqueous ammonium acetate solution of POPC-PDs (5 μM) at pH 6.8 (a) immediately after preparation of the solution and (d) after 3 h incubation. (b) and (e) Expanded viewes of the mass spectra shown in (a) and (d), respectively. (c) and (f) Zero-charge mass spectrum corresponding to (a) and (d), respectively.

Figure 4. Averaged structures of POPC-PDs obtained by MD simulations performed in solution over 50 ns (SapA shown as blue ribbon and POPC shown as sticks). (a) (SapA dimer + 10POPC) complex, (b) (SapA dimer + 26POPC) complex, (c) (SapA trimer + 33POPC) complex, and (d) (SapA tetramer + 42POPC) complex.

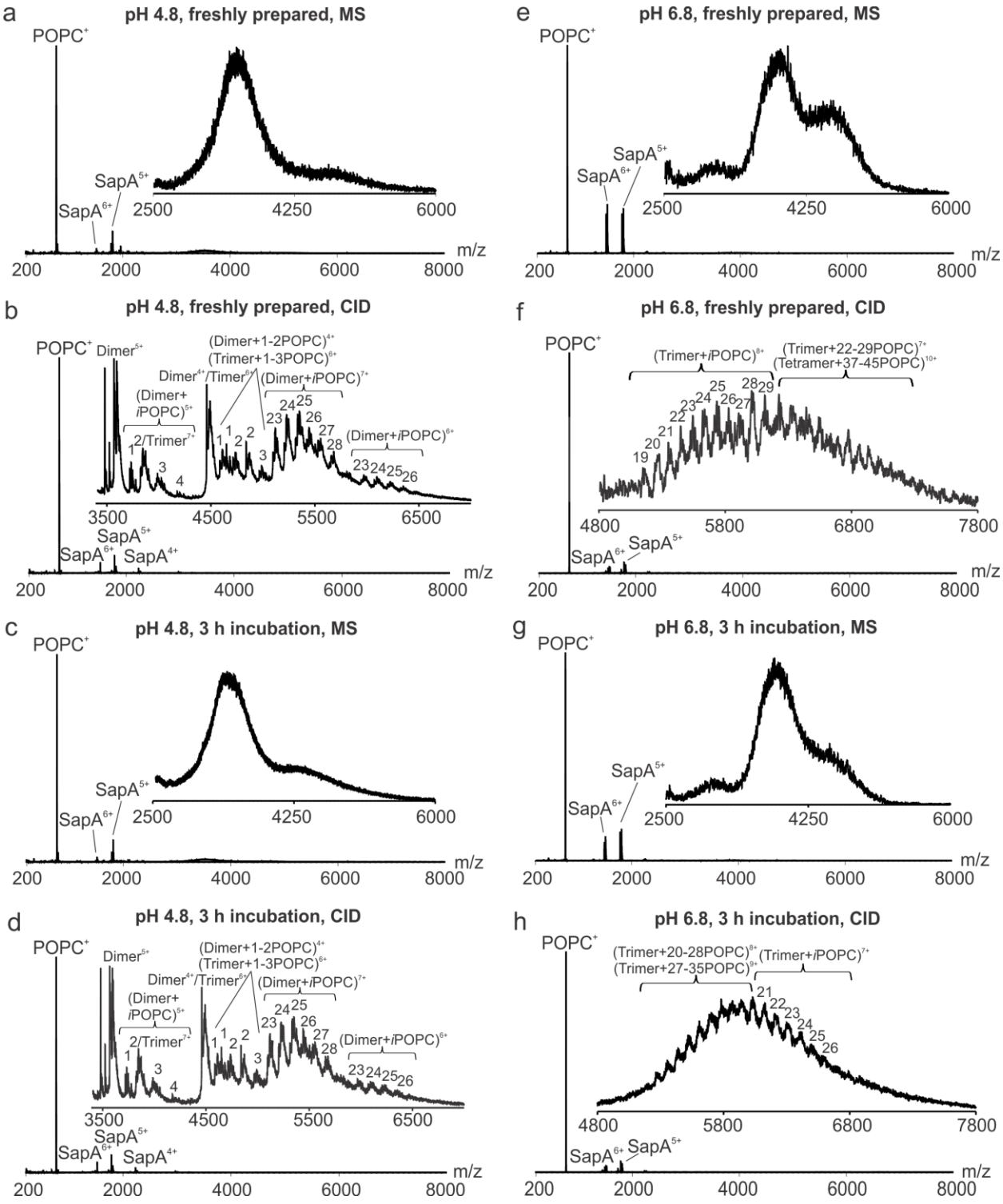
a
pH 4.8, freshly prepared, MS
POPC+
SapA5+
SapA6+
2500
4250
6000
m/z
200
2000
4000
6000
8000
e
pH 6.8, freshly prepared, MS
b
pH 4.8, freshly prepared, CID
Dimer5+
(Dimer+1-2POPC)4+
(Trimer+1-3POPC)6+
Dimer4+/Trimer6+
(Dimer+iPOPC)7+
(Dimer+iPOPC)5+
2/Trimer7+
(Dimer+iPOPC)6+
3500
4500
5500
6500
SapA4+
f
pH 6.8, freshly prepared, CID
(Trimer+iPOPC)8+
(Trimer+22-29POPC)7+
(Tetramer+37-45POPC)10+
4800
5800
6800
7800
c
pH 4.8, 3 h incubation, MS
g
pH 6.8, 3 h incubation, MS
d
pH 4.8, 3 h incubation, CID
h
pH 6.8, 3 h incubation, CID
(Trimer+20-28POPC)8+
(Trimer+27-35POPC)9+
(Trimer+iPOPC)7+

Figure 1

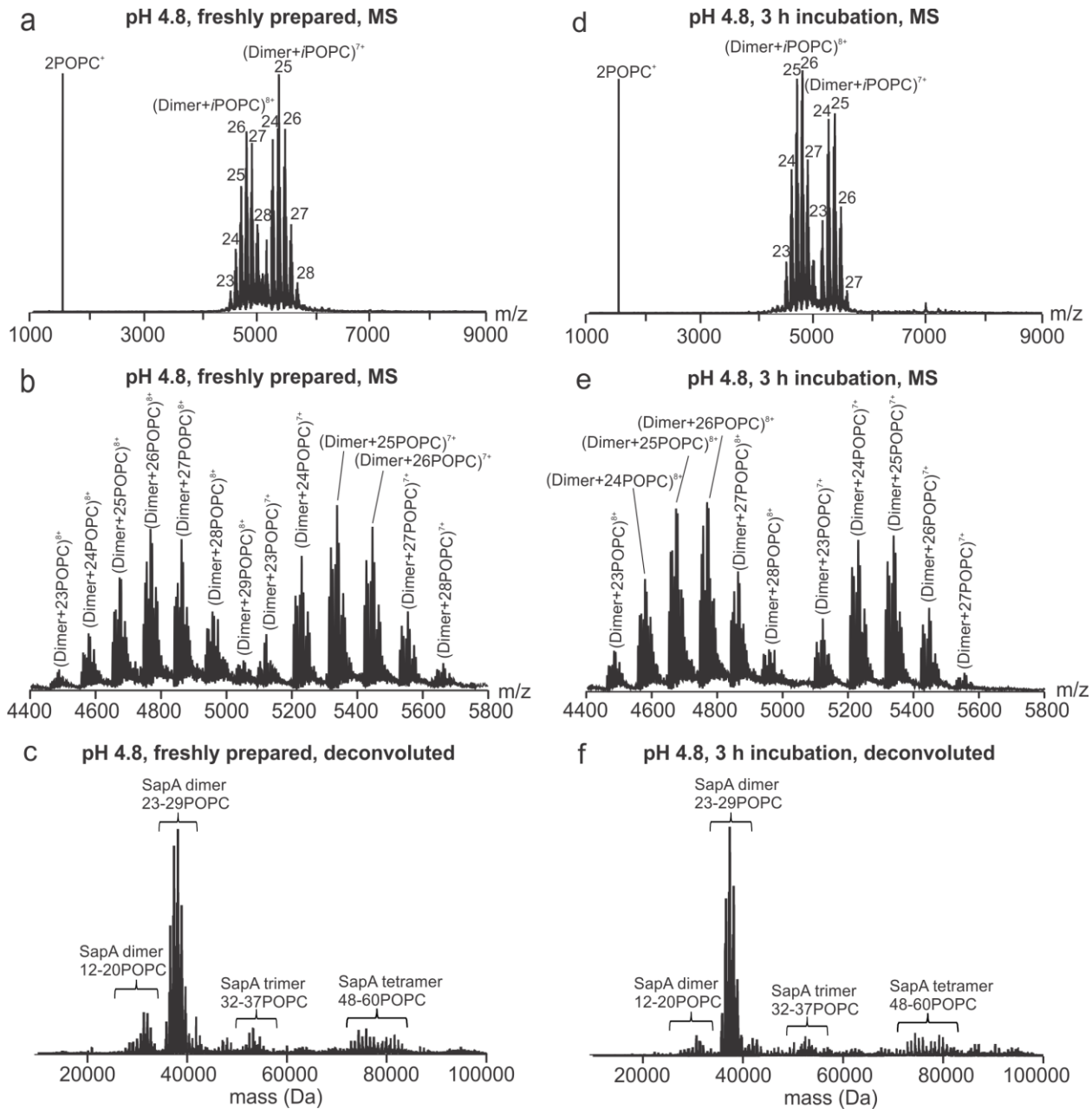
a
pH 4.8, freshly prepared, MS
2POPC+
(Dimer+iPOPC)7+
(Dimer+iPOPC)8+
m/z
b
pH 4.8, freshly prepared, MS
(Dimer+23POPC)8+
(Dimer+24POPC)8+
(Dimer+25POPC)8+
(Dimer+26POPC)8+
(Dimer+27POPC)8+
(Dimer+28POPC)8+
(Dimer+29POPC)8+
(Dimer+23POPC)7+
(Dimer+24POPC)7+
(Dimer+25POPC)7+
(Dimer+26POPC)7+
(Dimer+27POPC)7+
(Dimer+28POPC)7+
m/z
c
pH 4.8, freshly prepared, deconvoluted
SapA dimer
23-29POPC
SapA dimer
12-20POPC
SapA trimer
32-37POPC
SapA tetramer
48-60POPC
mass (Da)
d
pH 4.8, 3 h incubation, MS
2POPC+
(Dimer+iPOPC)8+
(Dimer+iPOPC)7+
m/z
e
pH 4.8, 3 h incubation, MS
(Dimer+23POPC)8+
(Dimer+24POPC)8+
(Dimer+25POPC)8+
(Dimer+26POPC)8+
(Dimer+27POPC)8+
(Dimer+28POPC)8+
(Dimer+23POPC)7+
(Dimer+24POPC)7+
(Dimer+25POPC)7+
(Dimer+26POPC)7+
(Dimer+27POPC)7+
m/z
f
pH 4.8, 3 h incubation, deconvoluted
SapA dimer
23-29POPC
SapA dimer
12-20POPC
SapA trimer
32-37POPC
SapA tetramer
48-60POPC
mass (Da)

Figure 2

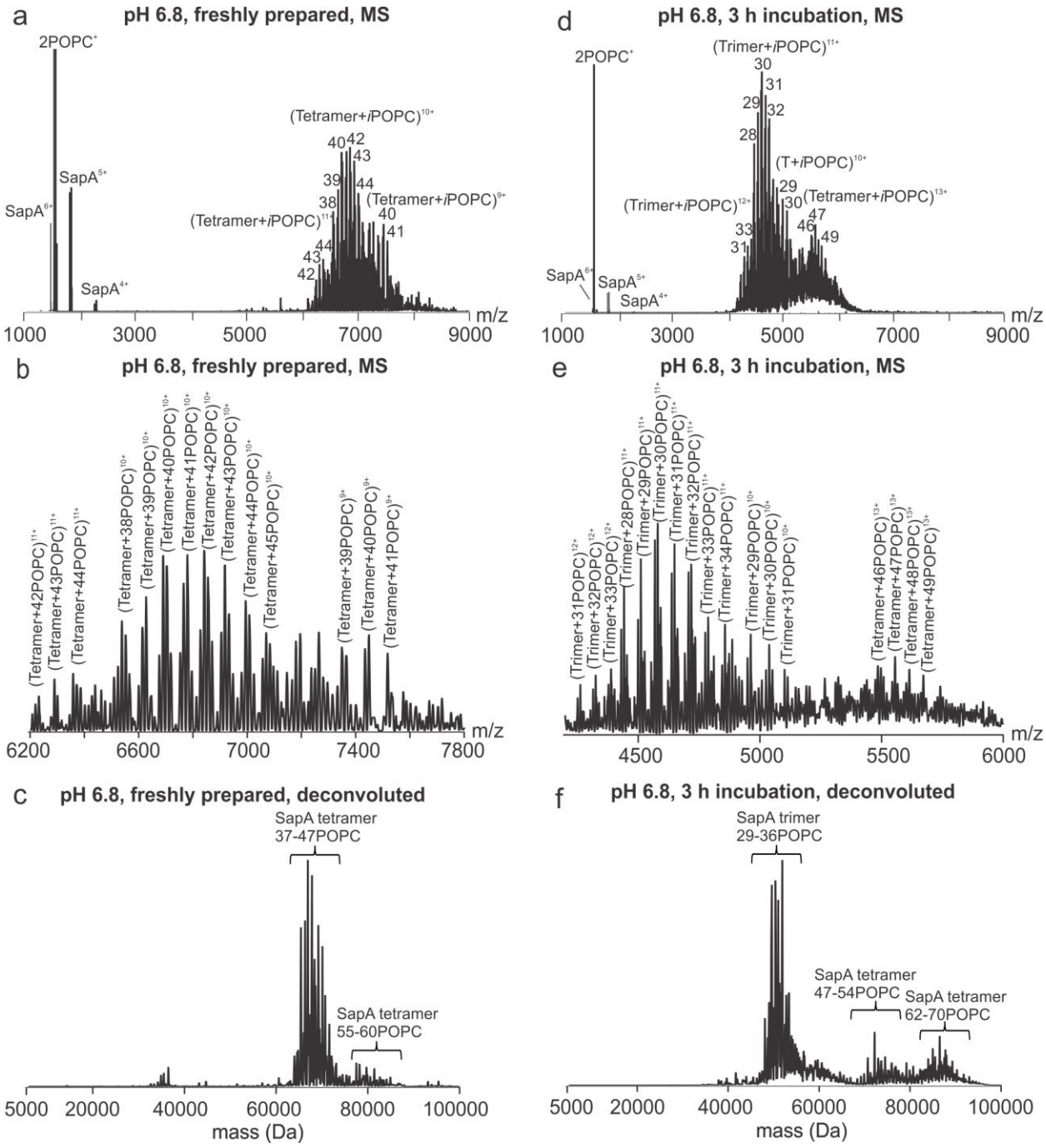
a
pH 6.8, freshly prepared, MS
2POPC+
SapA6+
SapA5+
SapA4+
(Tetramer+iPOPC)10+
(Tetramer+iPOPC)11+
(Tetramer+iPOPC)9+
m/z
1000
3000
5000
7000
9000
d
pH 6.8, 3 h incubation, MS
2POPC+
(Trimer+iPOPC)11+
(T+iPOPC)10+
(Trimer+iPOPC)12+
(Tetramer+iPOPC)13+
SapA6+
SapA5+
SapA4+
m/z
1000
3000
5000
7000
9000
b
pH 6.8, freshly prepared, MS
(Tetramer+42POPC)11+
(Tetramer+43POPC)11+
(Tetramer+44POPC)11+
(Tetramer+38POPC)10+
(Tetramer+39POPC)10+
(Tetramer+40POPC)10+
(Tetramer+41POPC)10+
(Tetramer+42POPC)10+
(Tetramer+43POPC)10+
(Tetramer+44POPC)10+
(Tetramer+45POPC)10+
(Tetramer+39POPC)9+
(Tetramer+40POPC)9+
(Tetramer+41POPC)9+
m/z
6200
6600
7000
7400
7800
e
pH 6.8, 3 h incubation, MS
(Trimer+31POPC)12+
(Trimer+32POPC)12+
(Trimer+33POPC)12+
(Trimer+28POPC)11+
(Trimer+29POPC)11+
(Trimer+30POPC)11+
(Trimer+31POPC)11+
(Trimer+32POPC)11+
(Trimer+33POPC)11+
(Trimer+34POPC)11+
(Trimer+29POPC)10+
(Trimer+30POPC)10+
(Trimer+31POPC)10+
(Tetramer+46POPC)13+
(Tetramer+47POPC)13+
(Tetramer+48POPC)13+
(Tetramer+49POPC)13+
m/z
4500
5000
5500
6000
c
pH 6.8, freshly prepared, deconvoluted
SapA tetramer
37-47POPC
SapA tetramer
55-60POPC
5000
20000
40000
60000
80000
100000
mass (Da)
f
pH 6.8, 3 h incubation, deconvoluted
SapA trimer
29-36POPC
SapA tetramer
47-54POPC
SapA tetramer
62-70POPC
5000
20000
40000
60000
80000
100000
mass (Da)

Figure 3

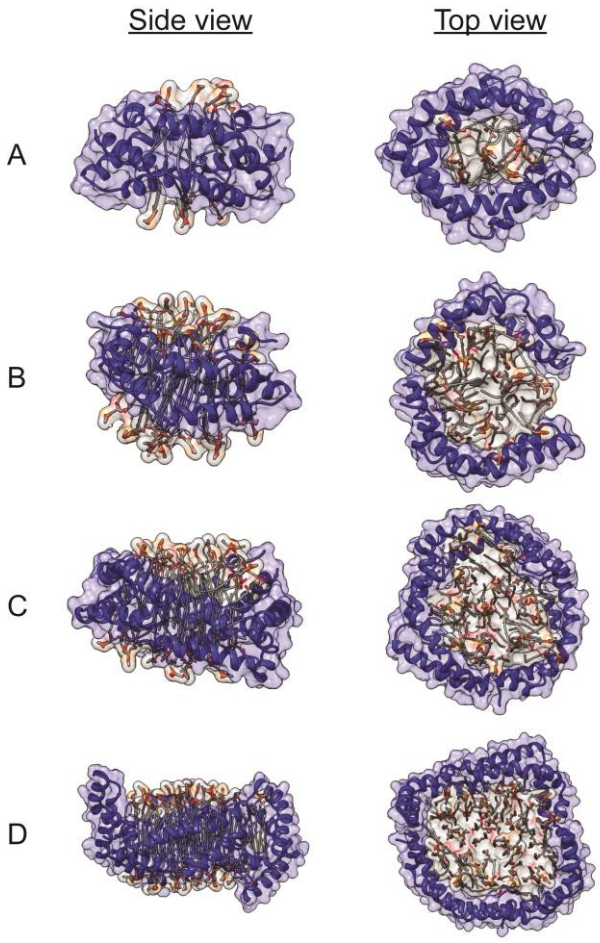

Figure 4

TOC graphic

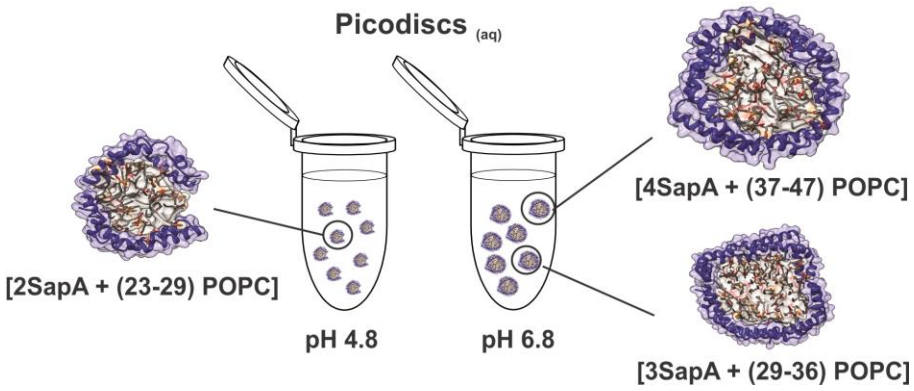
Picodiscs (aq)
[2SapA + (23-29) POPC]
pH 4.8
pH 6.8
[4SapA + (37-47) POPC]
[3SapA + (29-36) POPC]

SUPPORTING INFORMATION FOR:

Characterizing the Size and Composition of Saposin A Lipoprotein Picodiscs

Jun Li, Michele R. Richards, Dhanashri Bagal, Iain Campuzano, Elena N. Kitova, Zi Jian Xiong, Gilbert G. Privé and John S. Klassen

Table of Contents

Experimental

Mass Spectrometry

Exactive Plus Orbitrap. Instrument calibration was performed using a 25 μg μL^{-1} 50% (v/v) aqueous isopropanol solution of cesium iodide over the mass-to-charge ratio (*m/z*) range 1000 to 20,000. Nitrogen gas was used in the C-trap, as well as the HCD cell. Utilising a trapping gas pressure setting of 7.0 (software determined) the C-trap pressure is approximately $2x10^{-4}$ mbar and the pressure in the OrbiTrap analyser was $7.5x10^{-10}$ mbar. The voltage offsets on the transport multipoles were manually tuned to increase the transmission of large complexes (C-trap entrance lens; -2 V or 0 V, bent flatapole DC, 4 V; inter-flatapole DC, 4 V; injection flatapole DC, 4 V. Mass spectra were acquired under varying in-source CID voltage conditions ranging from 50 V to 200 V and varying HCD voltages from 20 V to 150 V to achieve efficient sample desolvation. The instrument was set at a nominal resolving power of 8,750 at *m/z* 200 and mass spectra were acquired for 1 min by averaging 10 microscans per one analytical scan.

Spectral deconvolution was performed with the UniDec[S1] deconvolution algorithm using the following parameters: *m/z* range – 4000 to 6000, however depending on the samples and observed *m/z* range, this range can vary; Subtract Curved - 10.0; Gaussian Smoothing - 1.0; Linear *m/z* (constant delta *m/z*); Bin every 1.0; Charge Range - 1 to 20; Mass range 10,000 to 100,000; Sample Mass Every 1.0 Da; Peak FWHM (Th) 4.0; Peak Shape Function - Gaussian; Charge Smooth Window - 0.0; Mass Difference - 760.0; Mass Smooth Window - 1.0; Maximum number of iterations - 1000. Spectral files were loaded as text files containing intensity and *m/z* values.

Collision Cross Section Analysis

The measured t_D values were corrected using eq 1:[S2]

$$t_D' = t_D - c\sqrt{m/z}/1000 - 10l_{transfer}/WV_{transfer} \quad (1)$$

where t_D' is the corrected drift time (in ms), t_D is the measured drift time (in ms), *m/z* is the mass-to-charge ratio of the observed ion and the constant *c* (enhanced duty cycle delay coefficient),[S2] $l_{transfer}$ is the length of the transfer T-wave region (in cm), and $WV_{transfer}$ is the transfer wave velocity (in m s^{-1}). The literature Ω (in N_2) values for the calibrant protein ions were corrected for charge and reduced mass (μ) by eq 2:[S2]

$$\Omega' = \Omega\sqrt{\mu}/z \quad (2)$$

where Ω′ is the corrected collision cross section in N_2 (nm^2), Ω is the literature collision cross section in N_2 (nm^2), μ and *z* is the reduced mass and charge of the observed ion. The final corrected drift times (t_D'') were calculated from eq 3:

$$t_D'' = (t_D')^X(z/\sqrt{\mu}) \quad (3)$$

where t_D'' is the final corrected drift times (in ms) and *X* is the exponential factor, which corresponds to the slope of the plot of ln(Ω′) versus ln(t_D'). The Ω values of the protonated PD ions were determined from the calibration curve of literature Ω values versus t_D''.

Molecular Dynamic (MD) Simulations

In all simulations, the ff03[S3] force field was used for SapA and the lipid11[S4] force field used for POPC. The time step for all simulations was 2 fs, and the temperature was maintained with the Berendsen[S5] (*ntt = 1*) thermostat with velocities rescaled every 1 ps. All bonds containing hydrogen were fixed using the SHAKE[S6] algorithm, except during the minimization step. To prepare the system for dynamics, the entire system was minimized, via 5000 steps of steepest descent followed by 5000 steps of conjugate gradient minimization. An equilibration period was carried out that included heating the system from 5 K to 300 K over 50 ps, then cooling to 5 K over 50 ps. This simulated annealing step was followed by a second, slower heating from 5 K to

300 K over 100 ps. The production simulation began after an additional 100 ps of equilibration at 300 K. Once the simulations were complete, R_g was calculated with AmberTools12,[S7] and for the gas-phase simulations, theoretical N_2-based Ω values were calculated using the Diffuse Hard Sphere Scattering method implemented in the IMoS suite of software[S8] using the following parameters: radgas 1.5; Mgas 28; Temperature 310; Nrotations EHSS 3; NgastotalEHSS 1000000; Accommodation 1.0; Diffuse 1; EHSS/DHSS 1. Coordinates were read in as PDB files.

Table S1. Composition of POPC-PDs. Comparison of theoretical and measured *m/z* values for signals observed in CID (Trap energy 50 V) mass spectrum (Figure 1b) acquired for a 200 mM aqueous ammonium acetate solution of POPC-PD (10 μM) at pH 4.8.

Composition	Theoretical *m/z*	Measured *m/z*	Composition	Theoretical *m/z*	Measured *m/z*
$(POPC + H)^{+}$	760.6	760.5	$(2SapA + 2POPC + 5H)^{5+}$	3898.0	3898.4
$(2POPC + H)^{+}$	1520.2	1520.1	$(2SapA + 3POPC + 5H)^{5+}$	4050.0	4050.2
$(SapA + 6H)^{6+}$	1486.0	1486.0	$(2SapA + 4POPC + 5H)^{5+}$	4202.0	4202.5
$(SapA + 6H)^{6+}$	1508.2	1508.2	$(2SapA + 4H)^{4+}$	4459.0	4459.2
$(SapA + 5H)^{5+}$	1784.2	1784.2	$(3SapA + 6H)^{6+}$	4459.0	
$(SapA + 5H)^{5+}$	1810.8	1810.8	$(3SapA + POPC + 6H)^{6+}$	4607.8	4608.4
$(SapA + 4H)^{4+}$	2230.0	2230.0	$(2SapA + POPC + 4H)^{4+}$	4649.0	4649.7
$(SapA + 4H)^{4+}$	2263.3	2263.3	$(3SapA + 2POPC + 6H)^{6+}$	4756.7	4756.7
$(SapA + POPC + 4H)^{4+}$	2420.0	2420.1	$(2SapA + 2POPC + 4H)^{4+}$	4839.0	4839.2
$(SapA + POPC + 4H)^{4+}$	2453.3	2453.4	$(3SapA + 3POPC + 6H)^{6+}$	4839.0	
$(SapA + 2POPC + 4H)^{4+}$	2610.0	2610.1	$(3SapA + 4POPC + 6H)^{6+}$	5010.0	5010.1
$(SapA + 2POPC + 4H)^{4+}$	2643.3	2643.3	$(2SapA + 3POPC + 4H)^{4+}$	5062.3	5062.5
$(SapA + 3POPC + 4H)^{4+}$	2800.0	2800.0	$(2SapA + 23POPC + 7H)^{7+}$	5120.1	5120.9
$(SapA + 3POPC + 4H)^{4+}$	2833.3	2833.3	$(2SapA + 24POPC + 7H)^{7+}$	5228.7	5228.8
$(SapA + 3H)^{3+}$	2973.0	2973.1	$(2SapA + 25POPC + 7H)^{7+}$	5337.3	5337.7
$(SapA + 3H)^{3+}$	3017.3	3017.4	$(2SapA + 26POPC + 7H)^{7+}$	5445.9	5445.2
$(SapA + POPC + 3H)^{3+}$	3226.3	3226.6	$(2SapA + 27POPC + 7H)^{7+}$	5554.4	5554.8
$(SapA + POPC + 3H)^{3+}$	3270.7	3270.3	$(2SapA + 28POPC + 7H)^{7+}$	5663.0	5662.8
$(SapA + 2POPC + 3H)^{3+}$	3479.7	3479.8	$(2SapA + 23POPC + 6H)^{6+}$	5973.3	5973.5
$(SapA + 2POPC + 3H)^{3+}$	3524.0	3523.9	$(2SapA + 24POPC + 6H)^{6+}$	6100.0	6100.1
$(2SapA + 5H)^{5+}$	3594.0	3594.1	$(2SapA + 25POPC + 6H)^{6+}$	6226.7	6226.1
$(2SapA + POPC + 5H)^{5+}$	3746.0	3746.2	$(2SapA + 26POPC + 6H)^{6+}$	6353.3	6353.5
$(3SapA + 7H)^{7+}$	3860.1	3860.5			

Table S2. Composition of POPC-PDs. Comparison of theoretical and measured *m/z* values for signals observed in CID (Trap energy 50 V) mass spectrum (Figure 1d) acquired for a 200 mM aqueous ammonium acetate solution of POPC-PD (10 μM) after 3 hours incubation at pH 4.8.

Composition	Theoretical *m/z*	Measured *m/z*	Composition	Theoretical *m/z*	Measured *m/z*
$(POPC + H)^{+}$	760.6	760.5	$(2SapA + 2POPC + 5H)^{5+}$	3898.0	3898.4
$(2POPC + H)^{+}$	1520.2	1520.1	$(2SapA + 3POPC + 5H)^{5+}$	4050.0	4050.2
$(SapA + 6H)^{6+}$	1486.0	1486.0	$(2SapA + 4POPC + 5H)^{5+}$	4202.0	4202.5
$(SapA + 6H)^{6+}$	1508.2	1508.2	$(2SapA + 4H)^{4+}$	4459.0	4459.2
$(SapA + 5H)^{5+}$	1784.2	1784.2	$(3SapA + 6H)^{6+}$	4459.0	
$(SapA + 5H)^{5+}$	1810.8	1810.8	$(3SapA + POPC + 6H)^{6+}$	4607.8	4608.4
$(SapA + 4H)^{4+}$	2230.0	2230.0	$(2SapA + POPC + 4H)^{4+}$	4649.0	4649.7
$(SapA + 4H)^{4+}$	2263.3	2263.3	$(3SapA + 2POPC + 6H)^{6+}$	4756.7	4756.7
$(SapA + POPC + 4H)^{4+}$	2420.0	2420.1	$(2SapA + 2POPC + 4H)^{4+}$	4839.0	4839.2
$(SapA + POPC + 4H)^{4+}$	2453.3	2453.4	$(3SapA + 3POPC + 6H)^{6+}$	4839.0	
$(SapA + 2POPC + 4H)^{4+}$	2610.0	2610.1	$(3SapA + 4POPC + 6H)^{6+}$	5010.0	5010.1
$(SapA + 2POPC + 4H)^{4+}$	2643.3	2643.3	$(2SapA + 3POPC + 4H)^{4+}$	5062.3	5062.5
$(SapA + 3POPC + 4H)^{4+}$	2800.0	2800.0	$(2SapA + 23POPC + 7H)^{7+}$	5120.1	5120.9
$(SapA + 3POPC + 4H)^{4+}$	2833.3	2833.3	$(2SapA + 24POPC + 7H)^{7+}$	5228.7	5228.8
$(SapA + 3H)^{3+}$	2973.0	2973.1	$(2SapA + 25POPC + 7H)^{7+}$	5337.3	5337.7
$(SapA + 3H)^{3+}$	3017.3	3017.4	$(2SapA + 26POPC + 7H)^{7+}$	5445.9	5445.2
$(SapA + POPC + 3H)^{3+}$	3226.3	3226.6	$(2SapA + 27POPC + 7H)^{7+}$	5554.4	5554.8
$(SapA + POPC + 3H)^{3+}$	3270.7	3270.3	$(2SapA + 28POPC + 7H)^{7+}$	5663.0	5662.8
$(SapA + 2POPC + 3H)^{3+}$	3479.7	3479.8	$(2SapA + 23POPC + 6H)^{6+}$	5973.3	5973.5
$(SapA + 2POPC + 3H)^{3+}$	3524.0	3523.9	$(2SapA + 24POPC + 6H)^{6+}$	6100.0	6100.1
$(2SapA + 5H)^{5+}$	3594.0	3594.1	$(2SapA + 25POPC + 6H)^{6+}$	6226.7	6226.1
$(2SapA + POPC + 5H)^{5+}$	3746.0	3746.2	$(2SapA + 26POPC + 6H)^{6+}$	6353.3	6353.5
$(3SapA + 7H)^{7+}$	3860.1	3860.5			

Table S3. Composition of POPC-PDs. Comparison of theoretical and measured *m/z* values for signals observed in CID (Trap energy 50 V) mass spectrum (Figure 1f) acquired for a 200 mM aqueous ammonium acetate solution of POPC-PD (10 μM) at pH 6.8.

Composition	Theoretical *m/z*	Measured *m/z*	Composition	Theoritical *m/z*	Measured *m/z*
$(POPC + H)^{+}$	760.6	760.6	$(3SapA + 23POPC + 8H)^{8+}$	5562.8	5561.4
$(2POPC + H)^{+}$	1520.2	1520.3	$(3SapA + 24POPC + 8H)^{8+}$	5657.8	5656.7
$(SapA + 6H)^{6+}$	1486.0	1486.0	$(3SapA + 25POPC + 8H)^{8+}$	5752.8	5752.5
$(SapA + 6H)^{6+}$	1508.2	1508.2	$(3SapA + 26POPC + 8H)^{8+}$	5847.8	5843.1
$(SapA + 5H)^{5+}$	1784.2	1784.2	$(3SapA + 27POPC + 8H)^{8+}$	5942.8	5942.4
$(SapA + 5H)^{5+}$	1810.8	1810.7	$(3SapA + 28POPC + 8H)^{8+}$	6037.8	6037.7
$(SapA + 4H)^{4+}$	2230.0	2230.0	$(3SapA + 29POPC + 8H)^{8+}$	6132.8	6133.2
$(SapA + 4H)^{4+}$	2263.3	2263.1	$(3SapA + 22POPC + 7H)^{7+}$	6248.7	6251.5
$(SapA + POPC + 4H)^{4+}$	2420.0	2420.0	$(3SapA + 23POPC + 7H)^{7+}$	6357.3	6356.8
$(SapA + POPC + 4H)^{4+}$	2453.3	2453.3	$(3SapA + 23POPC + 7H)^{7+}$	6376.3	6377.0
$(SapA + 2POPC + 4H)^{4+}$	2610.0	2610.1	$(4SapA + 37POPC + 10H)^{10+}$	6379.4	
$(SapA + 2POPC + 4H)^{4+}$	2643.3	2643.3	$(3SapA + 24POPC + 7H)^{7+}$	6465.9	6465.9
$(SapA + 3POPC + 4H)^{4+}$	2800.0	2800.0	$(4SapA + 38POPC + 10H)^{10+}$	6468.7	
$(SapA + 3POPC + 4H)^{4+}$	2833.3	2833.3	$(3SapA + 25POPC + 7H)^{7+}$	6555.4	6557.4
$(SapA + 3H)^{3+}$	2973.0	2973.1	$(4SapA + 39POPC + 10H)^{10+}$	6558.0	
$(SapA + 3H)^{3+}$	3017.3	3017.1	$(3SapA + 26POPC + 7H)^{7+}$	6645.0	6646.1
$(SapA + 4POPC + 4H)^{4+}$	2990.0	2990.2	$(4SapA + 40POPC + 10H)^{10+}$	6647.3	
$(SapA + 4POPC + 4H)^{4+}$	3023.3	3023.4	$(3SapA + 26POPC + 7H)^{7+}$	6702.0	6710.8
$(SapA + POPC + 3H)^{3+}$	3226.3	3226.6	$(4SapA + 41POPC + 10H)^{10+}$	6710.0	
$(SapA + POPC + 3H)^{3+}$	3270.7	3270.3	$(3SapA + 27POPC + 7H)^{7+}$	6810.6	6813.2
$(SapA + 2POPC + 3H)^{3+}$	3479.7	3479.9	$(4SapA + 42POPC + 10H)^{10+}$	6812.6	
$(SapA + 2POPC + 3H)^{3+}$	3524.0	3523.9	$(3SapA + 28POPC + 7H)^{7+}$	6862.1	6865.6
$(SapA + 3POPC + 3H)^{3+}$	3733.0	3733.3	$(4SapA + 43POPC + 10H)^{10+}$	6862.0	
$(SapA + 3POPC + 3H)^{3+}$	3777.3	3777.1	$(3SapA + 29POPC + 7H)^{7+}$	6970.7	6963.6
$(3SapA + 19POPC + 8H)^{8+}$	5182.8	5183.3	$(4SapA + 44POPC + 10H)^{10+}$	6964.6	
$(3SapA + 20POPC + 8H)^{8+}$	5277.8	5277.7	$(3SapA + 29POPC + 7H)^{7+}$	7027.7	7033.7
$(3SapA + 21POPC + 8H)^{8+}$	5372.8	5371.8	$(4SapA + 45POPC + 10H)^{10+}$	7027.3	
$(3SapA + 22POPC + 8H)^{8+}$	5467.8	5466.3			

Table S4. Composition of POPC-PDs. Comparison of theoretical and measured *m/z* values for signals observed in CID (Trap energy 50 V) mass spectrum (Figure 1h) acquired for a 200 mM aqueous ammonium acetate solution of POPC-PD (10 μM) after 3 hours incubation at pH 6.8.

Composition	Theoretical *m/z*	Measured *m/z*	Composition	Theoritical *m/z*	Measured *m/z*
$(POPC + H)^{+}$	760.6	760.6	$(3SapA + 21POPC + 8H)^{8+}$	5356.1	5354.3
$(2POPC + H)^{+}$	1520.2	1520.2	$(3SapA + 28POPC + 9H)^{9+}$	5352.2	
$(SapA + 5H)^{6+}$	1486.0	1486.0	$(3SapA + 22POPC + 8H)^{8+}$	5451.1	5453.0
$(SapA + 5H)^{6+}$	1508.2	1508.2	$(3SapA + 29POPC + 9H)^{9+}$	5451.4	
$(SapA + 5H)^{5+}$	1784.2	1784.3	$(3SapA + 23POPC + 8H)^{8+}$	5546.1	5539.6
$(SapA + 5H)^{5+}$	1810.8	1810.7	$(3SapA + 30POPC + 9H)^{9+}$	5535.9	
$(SapA + 4H)^{4+}$	2230.0	2230.0	$(3SapA + 24POPC + 8H)^{8+}$	5624.5	5621.2
$(SapA + 4H)^{4+}$	2263.3	2263.1	$(3SapA + 31POPC + 9H)^{9+}$	5620.3	
$(SapA + POPC + 4H)^{4+}$	2420.0	2420.0	$(3SapA + 25POPC + 8H)^{8+}$	5719.5	5723.3
$(SapA + POPC + 4H)^{4+}$	2453.3	2453.3	$(3SapA + 32POPC + 9H)^{9+}$	5719.6	
$(SapA + 2POPC + 4H)^{4+}$	2610.0	2610.1	$(3SapA + 26POPC + 8H)^{8+}$	5814.5	5806.2
$(SapA + 2POPC + 4H)^{4+}$	2643.3	2643.3	$(3SapA + 33POPC + 9H)^{9+}$	5804.0	
$(SapA + 3POPC + 4H)^{4+}$	2800.0	2800.0	$(3SapA + 26POPC + 8H)^{8+}$	5864.4	5860.7
$(SapA + 3POPC + 4H)^{4+}$	2833.3	2833.3	$(3SapA + 34POPC + 9H)^{9+}$	5858.9	
$(SapA + 3H)^{3+}$	2973.0	2973.1	$(3SapA + 27POPC + 8H)^{8+}$	5926.1	5928.5
$(SapA + 3H)^{3+}$	3017.3	3017.3	$(3SapA + 35POPC + 9H)^{9+}$	5928.6	
$(SapA + 4POPC + 4H)^{4+}$	2990.0	2990.2	$(3SapA + 28POPC + 8H)^{8+}$	6037.8	6037.5
$(SapA + 4POPC + 4H)^{4+}$	3023.3	3023.4	$(3SapA + 21POPC + 7H)^{7+}$	6140.1	6140.8
$(SapA + POPC + 3H)^{3+}$	3226.3	3226.6	$(3SapA + 22POPC + 7H)^{7+}$	6248.7	6248.7
$(SapA + POPC + 3H)^{3+}$	3270.7	3270.3	$(3SapA + 23POPC + 7H)^{7+}$	6338.3	6337.9
$(SapA + 2POPC + 3H)^{3+}$	3479.7	3479.9	$(3SapA + 24POPC + 7H)^{7+}$	6465.9	6465.6
$(SapA + 2POPC + 3H)^{3+}$	3524.0	3523.9	$(3SapA + 25POPC + 7H)^{7+}$	6574.4	6572.2
$(SapA + 3POPC + 3H)^{3+}$	3733.0	3733.3	$(3SapA + 26POPC + 7H)^{7+}$	6664.0	6663.3
$(SapA + 3POPC + 3H)^{3+}$	3777.3	3777.1	$(3SapA + 21POPC + 8H)^{8+}$	5356.1	5354.3
$(3SapA + 20POPC + 8H)^{8+}$	5277.8	5278.1			
$(3SapA + 27POPC + 9H)^{9+}$	5282.6				

Table S5. Measured drift times (t_D), corrected drift times (t_D' and t_D'') and collisional cross sections (Ω) for (SapA dimer + *i*POPC)$^{n+}$ ions.

Charge state (n)	m/z	Drift time (t_D, ms)	Corrected drift time (t_D', ms)	Final corrected drift time (t_D'', ms)	Calculated Ω (nm^2)
11	3286.5	8.75	8.40	4.03	29.32
11	3353.6	9.18	8.83	4.09	29.78
11	3412.5	9.35	9.00	4.12	29.95
11	3480.1	9.48	9.13	4.14	30.08
11	3556.4	9.67	9.32	4.16	30.27
11	3621.3	9.87	9.52	4.19	30.47
10	3681.3	10.82	10.46	3.92	28.55
10	3740.0	10.99	10.63	3.94	28.69
10	3809.9	11.24	10.88	3.97	28.90
10	3883.1	11.51	11.15	4.00	29.12
10	3950.0	11.72	11.36	4.02	29.28
10	4019.9	12.13	11.77	4.07	29.60

Table S6. Measured drift times (t_D), corrected drift times (t_D' and t_D'') and collisional cross sections (Ω) for (SapA tetramer + *i*POPC)$^{n+}$.

Charge state	m/z	Drift time (t_D, ms)	Corrected drift time (t_D', ms)	Final corrected drift time (t_D'', ms)	Calculated Ω (nm^2)
17	3867.8	11.26	10.90	6.75	48.92
17	3936.1	11.59	11.23	6.82	49.38
17	4012.1	11.83	11.47	6.86	49.70
17	4059.6	11.95	11.59	6.88	49.86
17	4105.0	12.09	11.73	6.91	50.04
17	4158.8	12.18	11.82	6.93	50.16
16	4213.0	12.98	12.62	6.65	48.19
16	4263.1	13.26	12.90	6.70	48.52
16	4316.2	13.63	13.27	6.76	48.94
16	4366.1	13.88	13.52	6.80	49.23
16	4410.3	14.09	13.73	6.83	49.46
15	4578.7	15.55	15.18	6.61	47.86
15	4628.4	16.08	15.71	6.68	48.37
15	4681.2	16.32	15.95	6.71	48.60
15	4732.7	16.64	16.27	6.75	48.89
14	4832.1	17.62	17.25	6.41	46.49
14	4896.3	17.99	17.62	6.46	46.79
14	4942.7	18.27	17.90	6.49	47.02
14	5000.3	18.46	18.09	6.51	47.17

Table S7. Measured drift times (t_D), corrected drift times (t_D' and t_D'') and collisional cross sections (Ω) for (SapA trimer + *i*POPC)$^{n+}$.

Charge state	m/z	Drift time (t_D, ms)	Corrected drift time (t_D', ms)	Final corrected drift time (t_D'', ms)	Calculated Ω (nm^2)
13	3794.6	11.03	10.67	5.13	37.25
13	3850.3	11.20	10.84	5.16	37.43
13	3910.5	11.24	10.88	5.16	37.47
13	3965.6	11.25	10.89	5.16	37.48
13	4034.2	11.52	11.16	5.20	37.76
13	4082.3	11.93	11.57	5.26	38.18
12	4140.6	12.51	12.15	4.93	35.81
12	4200.8	12.75	12.39	4.96	36.02
12	4264.3	13.07	12.71	5.00	36.31
12	4377.1	13.49	13.13	5.05	36.67
12	4394.8	13.81	13.45	5.09	36.94
12	4452.3	14.27	13.91	5.14	37.33

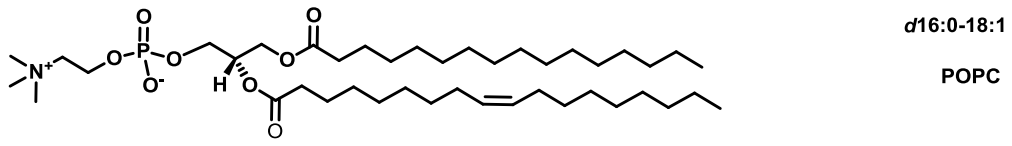

Figure S1. Structure of 1-palmitoyl-2-oleoyl-*sn*-glycero-3-phosphocholine (POPC).

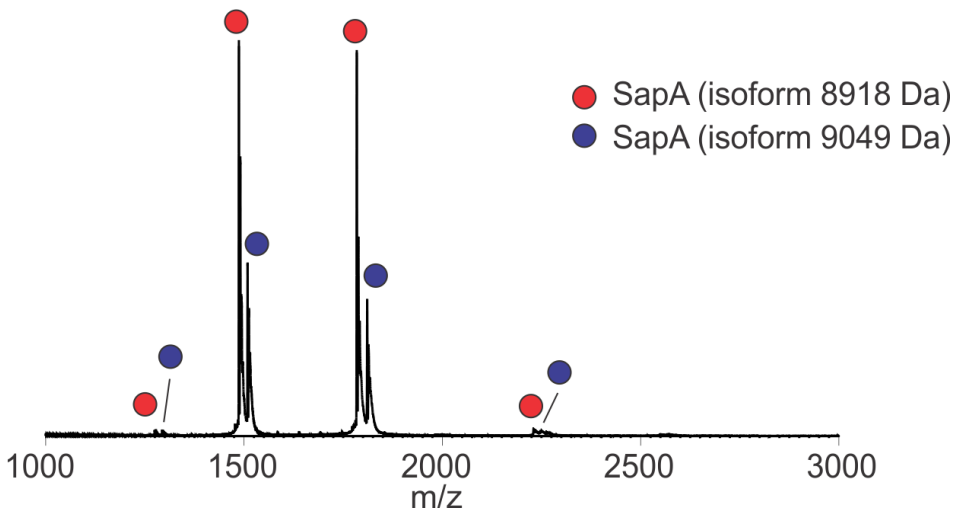

Figure S2. ESI mass spectrum acquired for SapA (10 µM) in a 200 mM aqueous ammonium acetate solution at pH 6.8.

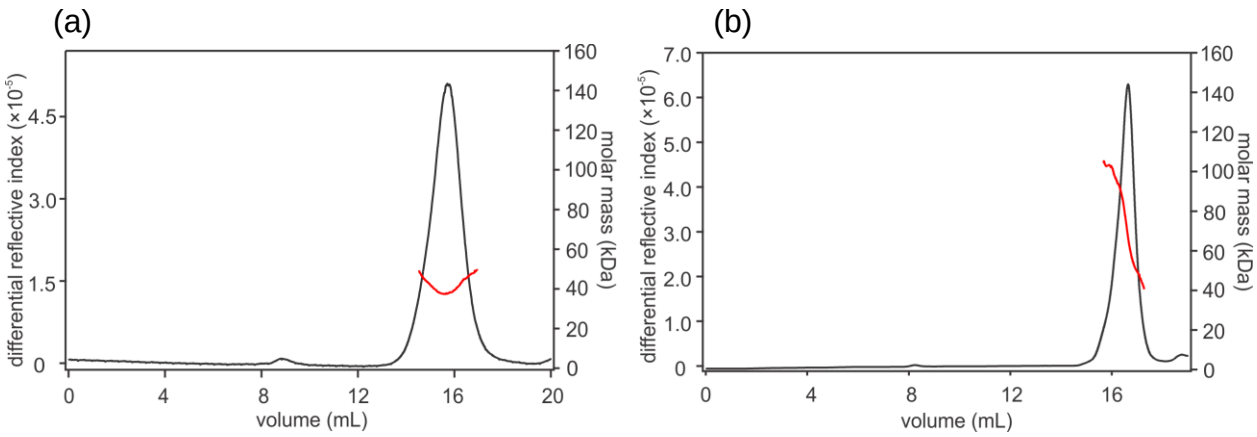

Figure S3. SEC-MALLS analysis of POPC-PDs (225 μM) solution in 200 mM ammonium acetate at (a) pH 4.8 or (b) 6.8. The black line represents the SEC elution profile monitored by refractive index and the red line across the elution peak indicates the MW calculated by MALLS.

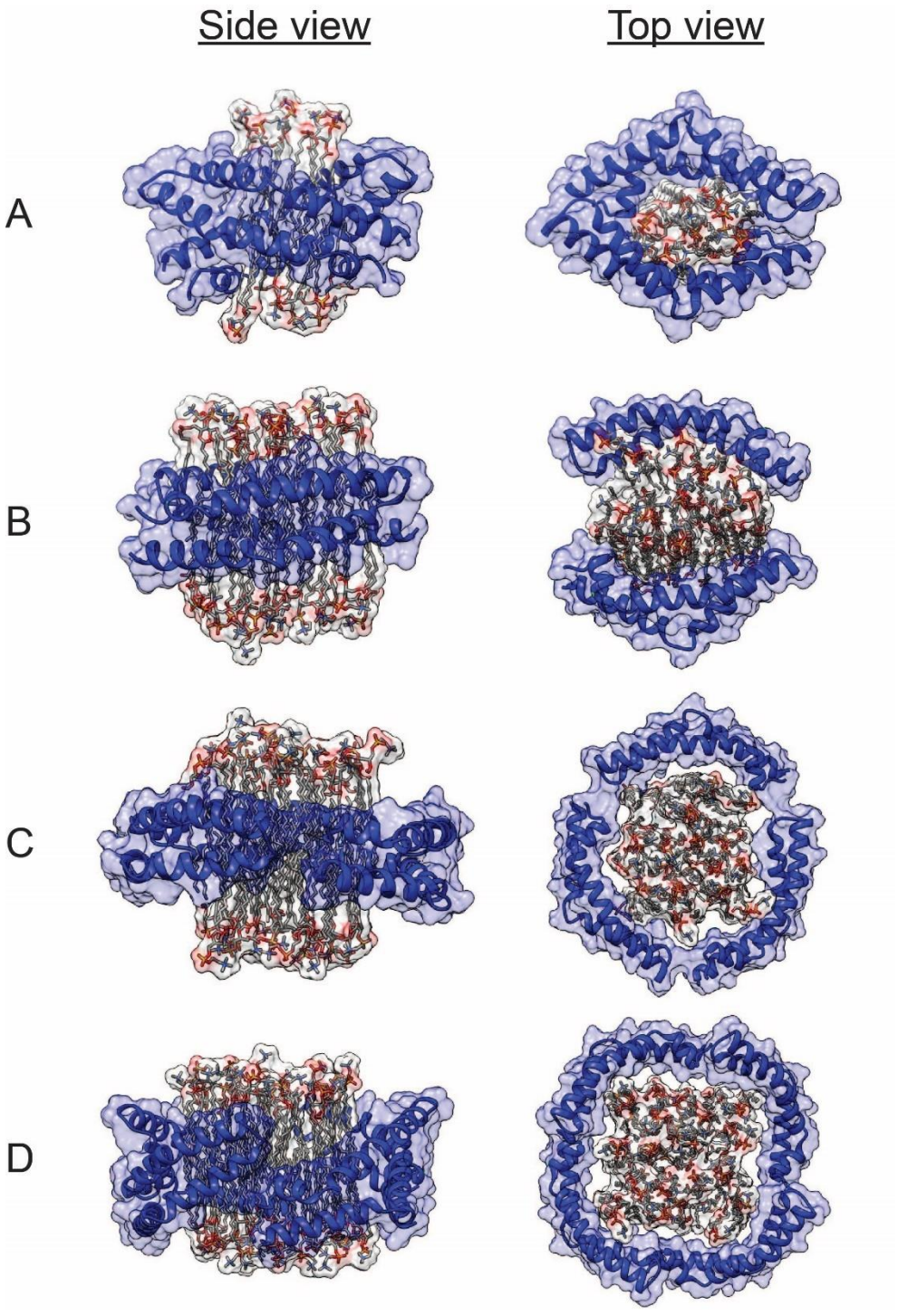

Figure S4. Initial configurations of POPC-PDs used for the solution MD simulations - (a) (SapA dimer + 10POPC) complex, (b) (SapA dimer + 26POPC) complex, (c) (SapA trimer + 33POPC) complex, and (d) (SapA tetramer + 42POPC) complex. SapA proteins are shown as blue ribbons and POPC molecules are shown as sticks.

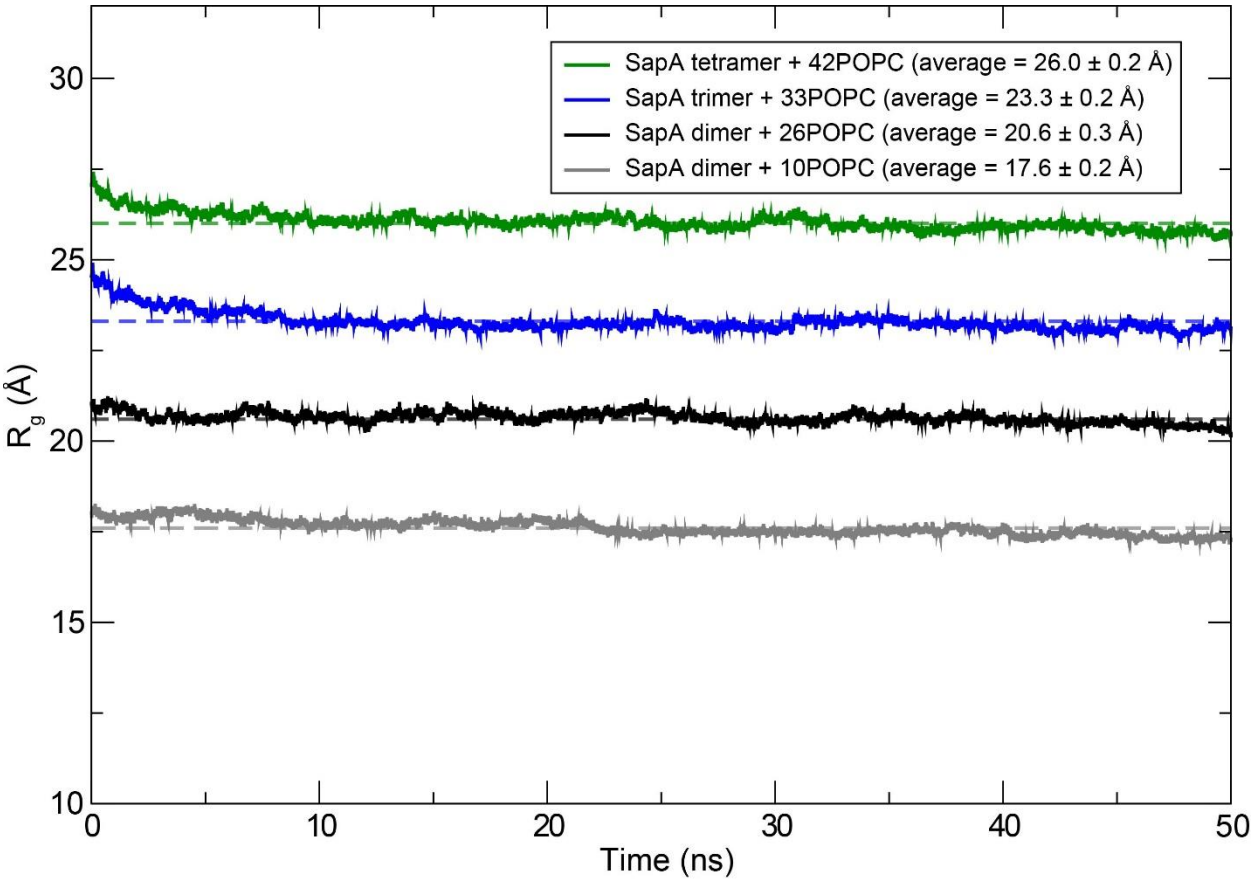

Figure S5. Radius of gyration (R_g) for the 50-ns solution MD simulations. The (SapA dimer + 10POPC) complex is shown in grey, (SapA dimer + 26POPC) complex is shown in in black, the (SapA trimer + 33POPC) complex is shown in blue, and the (SapA tetramer + 42POPC) complex is shown in green. The average R_g values, determined over the course of the simulations, are shown as dashed lines – (SapA dimer + 10POPC), R_g = 17.6 ± 0.2 Å; (SapA dimer + 26POPC), R_g = 20.6 ± 0.2 Å; (SapA trimer + 33POPC), R_g = 23.3 ± 0.3 Å; and (SapA tetramer + 42POPC), R_g = 26.0 ± 0.2 Å.

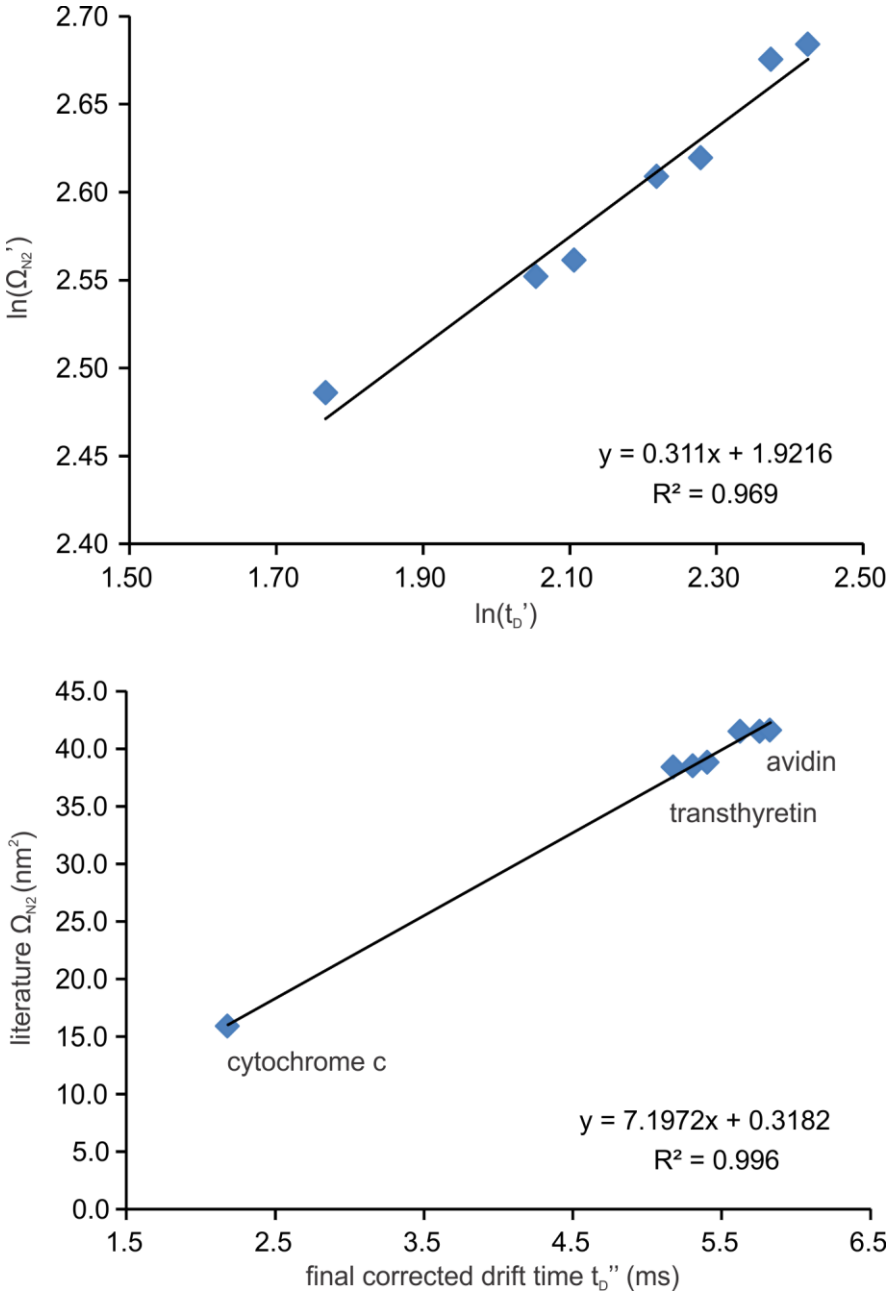

Figure S6. (a) Plot of $\ln(\Omega_{N2}')$ versus $\ln(t_D')$ for the calibrants: cytochrome c, transthyretin and avidin. An exponential factor (*X*) of 0.311 was determined from the slope of the plot. (b) Calibration displayed as a linear plot of literature Ω_{N2} values and final corrected drift times (t_D'').

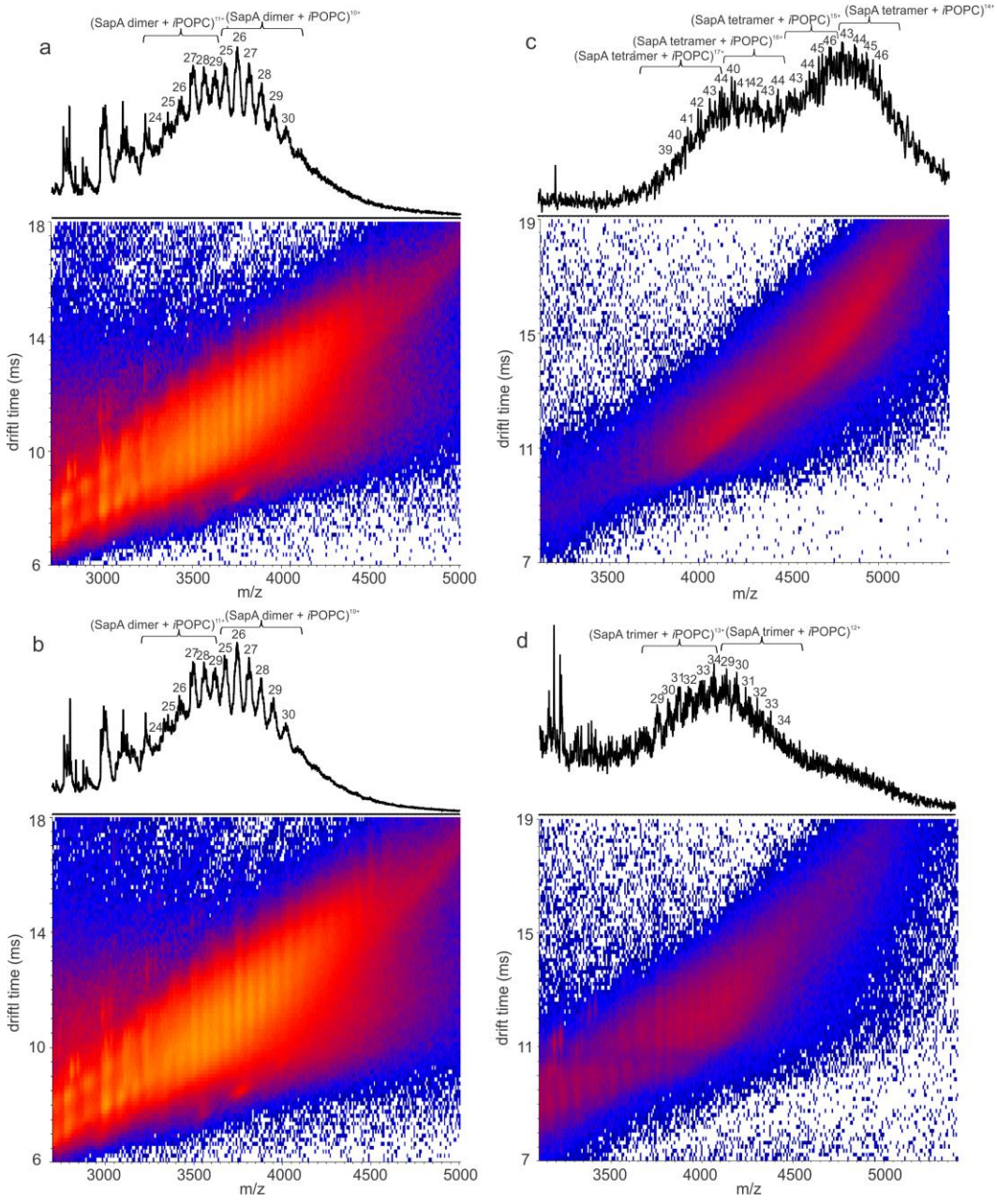

Figure S7. ESI mass spectra and corresponding IMS heat maps (*m/z* versus IMS drift times) measured in positive ion mode for (a) freshly prepared 200 mM aqueous ammonium acetate solutions (pH 4.8) of POPC-PDs (10 µM) and (b) after 3 h incubation. ESI mass spectra and corresponding IMS heat maps measured in positive ion mode for (c) freshly prepared 200 mM aqueous ammonium acetate solutions (pH 6.8) of POPC-PDs (10 µM) and (d) after 3 h incubation.

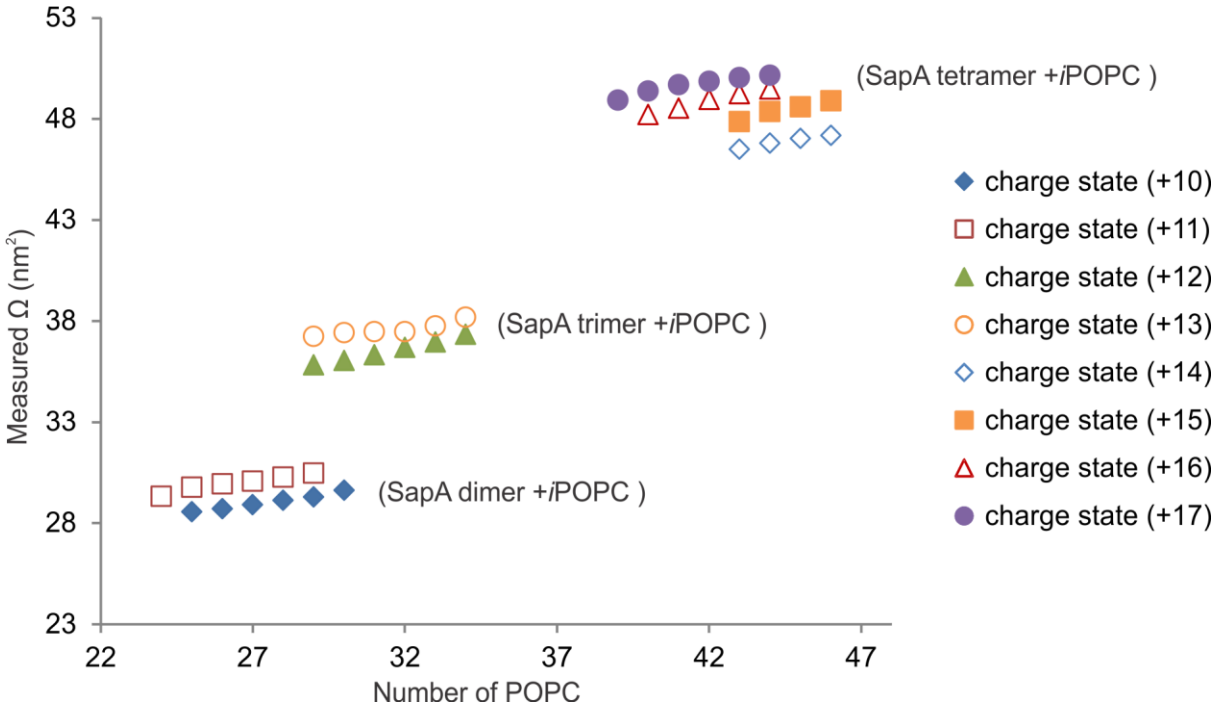

Figure S8. Measured Ω values plotted versus composition (number of POPC) at given charge states for POPC-PD ions: (SapA dimer + *i*POPC)$^{n+}$ ions, (SapA trimer + *i*POPC)$^{n+}$ ions, and (SapA tetramer + *i*POPC)$^{n+}$ ions.

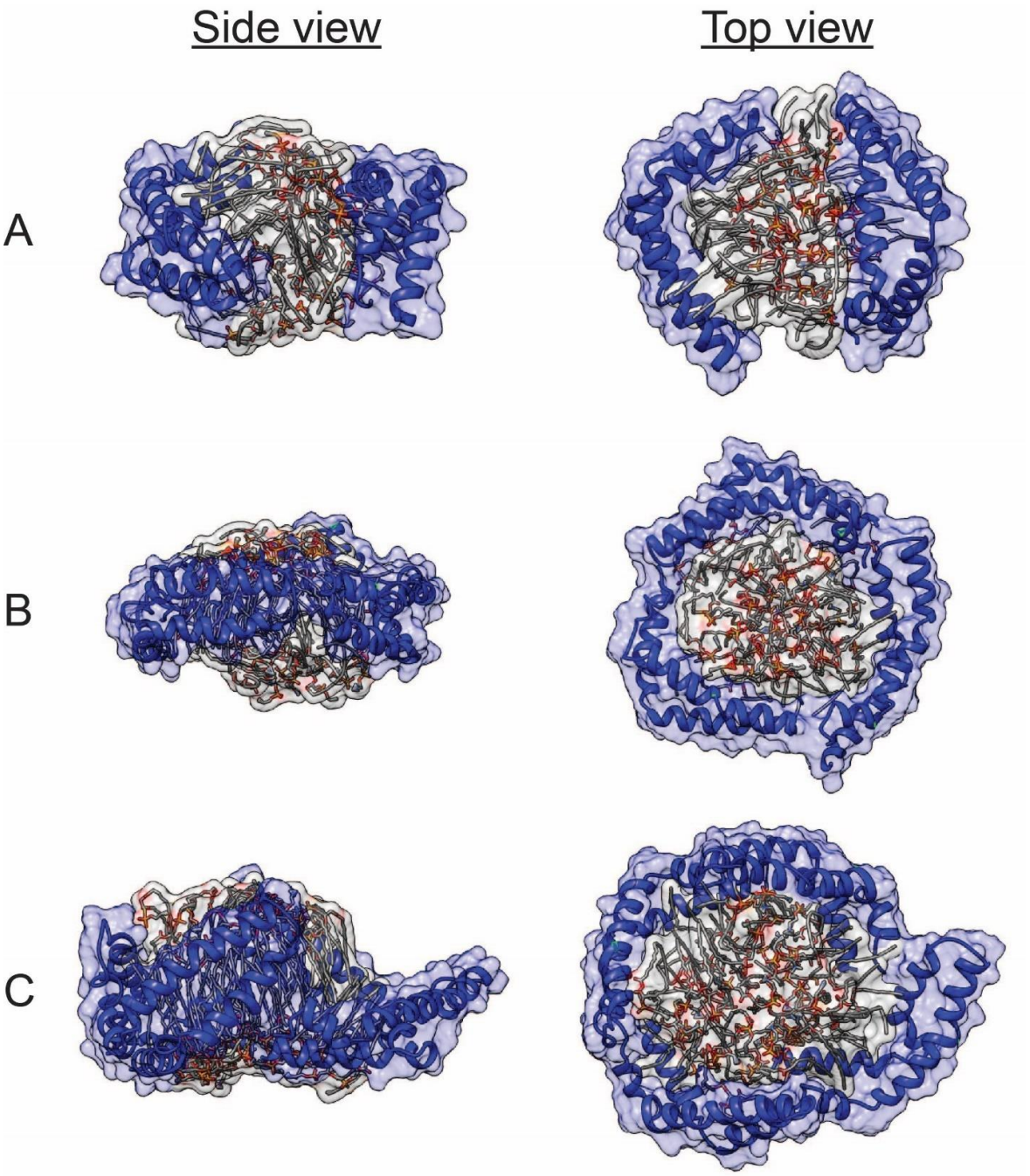

Figure S9. The averaged structures of the POPC-PD complexes from 20-ns gas-phase MD simulations. (a) (SapA dimer + 26POPC)$^{8+}$ ion, (b) (SapA trimer + 33POPC)$^{12+}$ ion, and (c) (SapA tetramer + 42POPC)$^{16+}$ ion.

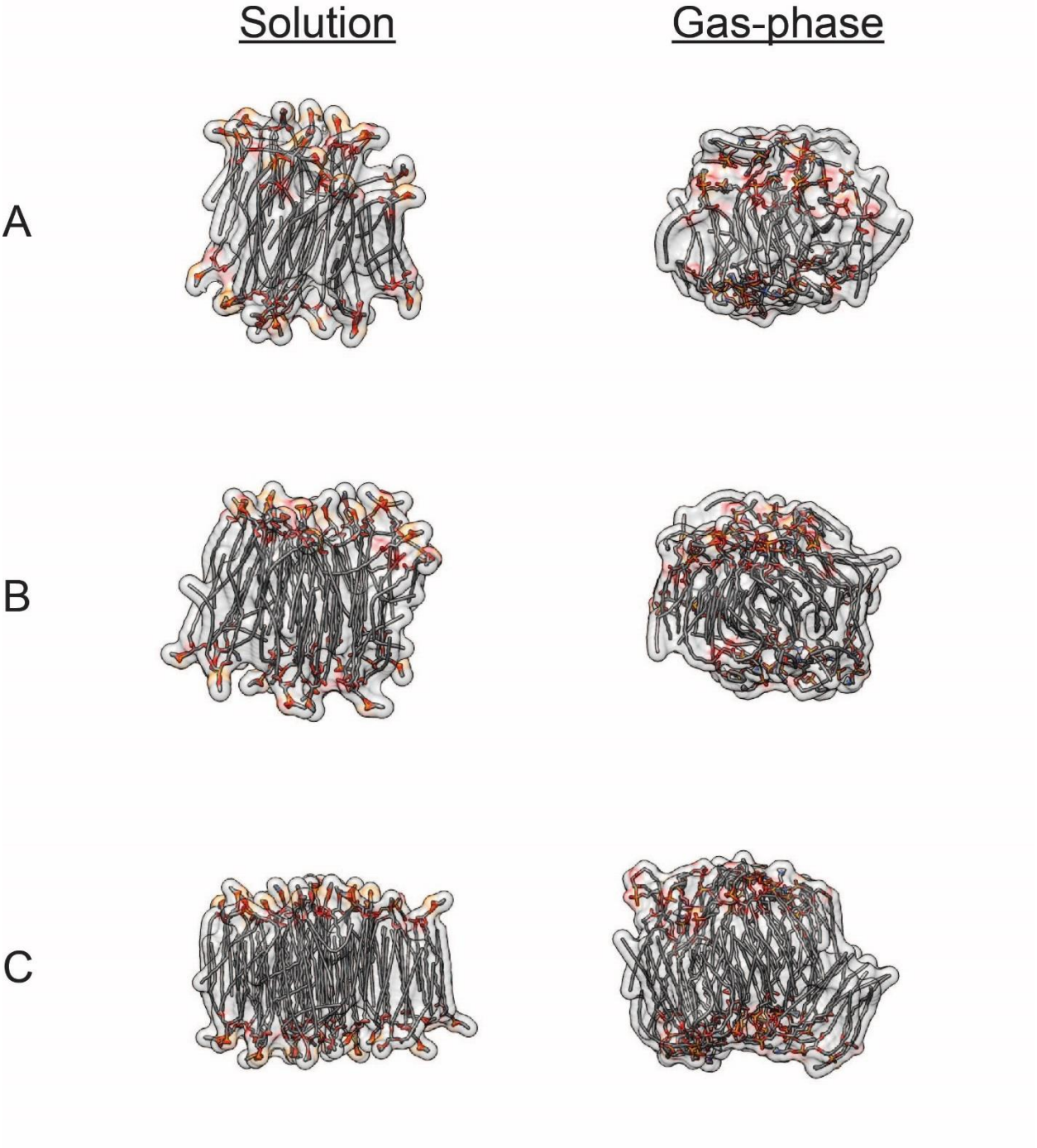

Figure S10. The averaged lipid conformations for POPC-PDs complexes from solution and gas-phase MD simulations - (a) (SapA dimer + 26POPC), (b) (SapA trimer + 33POPC) ion, and (c) (SapA tetramer + 42POPC). The gas-phase simulations were performed on the (a) $(\text{SapA dimer + 26POPC})^{8+}$, (b) $(\text{SapA trimer + 33POPC})^{12+}$ and (c) $(\text{SapA tetramer + 42POPC})^{16+}$ ions.

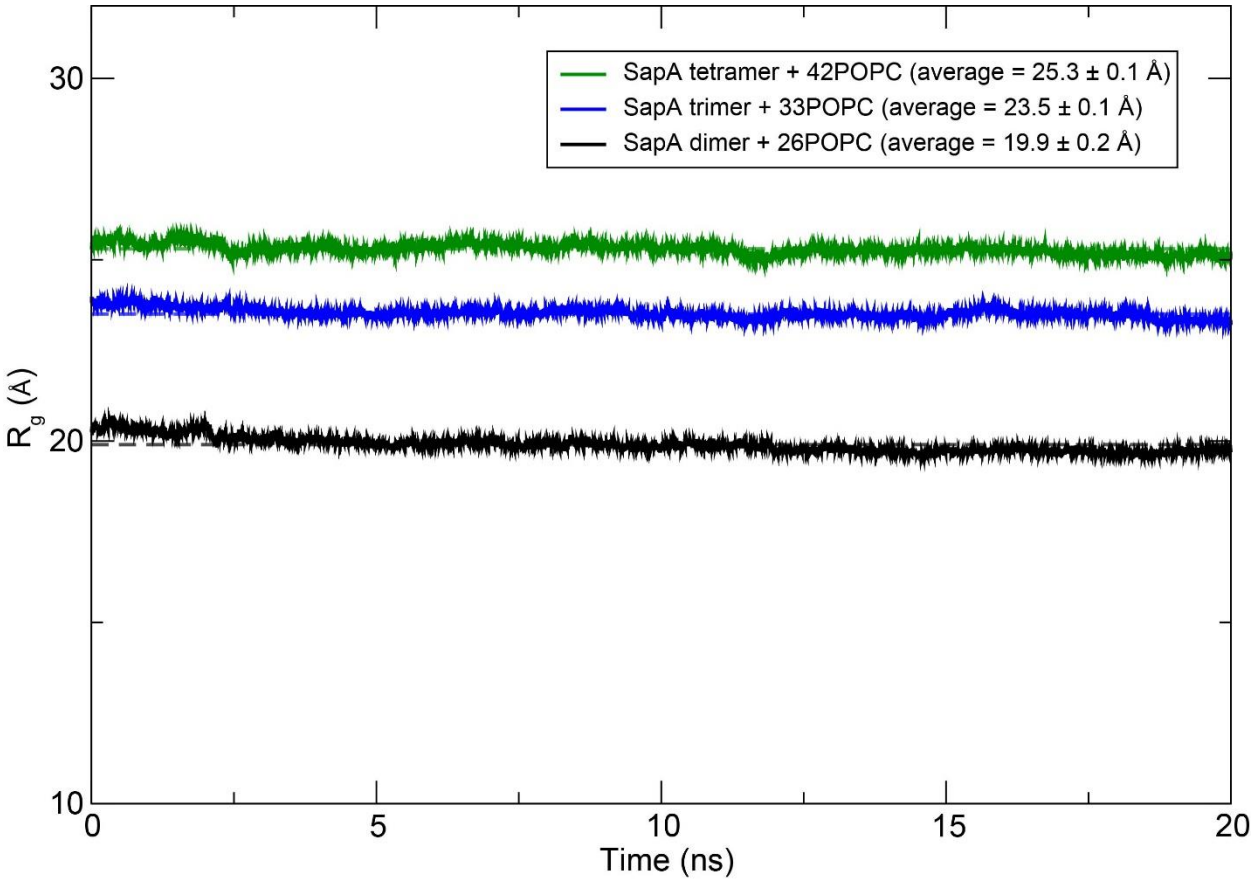

Figure S11. Radius of gyration (R_g) for the 20-ns gas-phase MD simulations. Results for the (SapA dimer + 26POPC)$^{8+}$ ion is shown in black, the (SapA trimer + 33POPC)$^{12+}$ ion is shown in blue, and the (SapA tetramer + 42POPC)$^{16+}$ ions is shown in green. The average R_g values, determined over the course of the simulations, are shown as dashed lines – (SapA dimer + 26POPC), R_g = 19.9 ± 0.2 Å; (SapA trimer + 33POPC), R_g = 23.5 ± 0.1 Å; and (SapA tetramer + 42POPC), R_g = 25.3 ± 0.1 Å.

References

S1. Marty, M. T.; Baldwin, A. J.; Marklund, E. G.; Hochberg, G. K.; Benesch, J. L.; Robinson, C. V. *Anal. Chem.* **2015**, *87*, 4370-4376.

S2. Ruotolo, B. T.; Benesch, J. L. P.; Sandercock, A. M.; Hyung, S. J.; Robinson, C. V. *Nat. Protoc*. **2008**, *3*, 1139−1152.

S3. Duan, Y.; Wu, C.; Chowdhury, S.; Lee, M. C.; Xiong, G.; Zhang, W.; Yang, R.; Cieplak, P.; Luo, R.; Lee, T.; Caldwell, J.; Wang, J.; Kollman, P. *J. Comput. Chem*. **2003**, *24*, 1999−2012.

S4. Skjevik, Å. A.; Madej, B. D.; Walker, R. C.; Teigen, K. *J. Phys. Chem. B* **2012**, *116*, 11124−11136.

S5. Berendsen, H. J. C.; Postma, J. P. M.; Gunsteren, W. F. v.; DiNola, A.; Haak, J. R. *J. Chem. Phys*. **1984**, *81*, 3684–3690.

S6. Ryckaert, J.-P.; Ciccotti, G.; Berendsen, H. J. C. *J. Comput. Phys*. **1977**, *23*, 327–341.

S7. Contributors to Amber. http://ambermd.org/contributors.html (accessed 1/26/2016).

S8. Larriba, C.; Hogan, C. J. Jr. *J. Phys. Chem. A* **2013**, *117*, 3887-3901.